doi:10.1093/brain/aww113 BRAIN 2016: 139; 1939–1957 | 1939

BRAIN
A JOURNAL OF NEUROLOGY

IL-10-dependent Tr1 cells attenuate astrocyte activation and ameliorate chronic central nervous system inflammation

Lior Mayo,[1,2] Andre Pires Da Cunha,[1] Asaf Madi,[3] Vanessa Beynon,[1] Zhiping Yang,[4] Jorge I. Alvarez,[5,6] Alexandre Prat,[5] Raymond A. Sobel,[7] Lester Kobzik,[4] Hans Lassmann,[8] Francisco J. Quintana[1] and Howard L. Weiner[1]

See Winger and Zamvil (doi:10.1093/brain/aww121) for a scientific commentary on this article.

The innate immune system plays a central role in the chronic central nervous system inflammation that drives neurological disability in progressive forms of multiple sclerosis, for which there are no effective treatments. The mucosal immune system is a unique tolerogenic organ that provides a physiological approach for the induction of regulatory T cells. Here we report that nasal administration of CD3-specific antibody ameliorates disease in a progressive animal model of multiple sclerosis. This effect is IL-10-dependent and is mediated by the induction of regulatory T cells that share a similar transcriptional profile to Tr1 regulatory cells and that suppress the astrocyte inflammatory transcriptional program. Treatment results in an attenuated inflammatory milieu in the central nervous system, decreased microglia activation, reduced recruitment of peripheral monocytes, stabilization of the blood–brain barrier and less neurodegeneration. These findings suggest a new therapeutic approach for the treatment of progressive forms of multiple sclerosis and potentially other types of chronic central nervous system inflammation.

1 Ann Romney Center for Neurologic Diseases, Brigham and Women's Hospital, Harvard Medical School, Boston, MA, USA
2 Cell Research and Immunology Department, Sagol School of Neuroscience, George S. Wise Faculty of Life Sciences, Tel Aviv University, Tel Aviv 699788, Israel
3 Evergrande Center for Immunologic Diseases, Harvard Medical School, Brigham and Women's Hospital, Boston, MA 02115, USA
4 Environmental Health Department, Harvard T. H. Chan School of Public Health, Boston, MA 02115, USA
5 Neuroimmunology Research Lab, CRCHUM, Faculty of Medicine, Université de Montréal, Montréal, QC, Canada
6 Pathobiology Department, University of Pennsylvania, Philadelphia, PA 19104, USA
7 Stanford University School of Medicine, Stanford, USA
8 Center for Brain Research, Medical University of Vienna, Spitalgasse 4, A-1090 Wien, Austria

Correspondence to: Howard L. Weiner,
Ann Romney Center for Neurologic Diseases, Brigham and Women's Hospital,
Harvard Medical School,
77 Avenue Louis Pasteur,
HIM 730,
Boston, MA 02115,
USA
E-mail: hweiner@rics.bwh.harvard.edu

Keywords: astrocyte; neuroinflammation; multiple sclerosis; T-lymphocytes; interleukin 10

Abbreviations: EAE = experimental autoimmune encephalomyelitis; GFP = green fluorescent protein; LAP = latency-associated peptide; mAb = monoclonal antibody; Tr1 = type 1 regulatory

Received July 22, 2015. Revised March 13, 2016. Accepted March 21, 2016. Advance Access publication May 31, 2016

Introduction

Multiple sclerosis is a chronic, inflammatory, demyelinating disease of the CNS. Approximately 85% of patients with multiple sclerosis initially exhibit a relapsing-remitting clinical course of the disease in which autoimmune attacks lead to impaired neurological function that are followed by periods of recovery. Many patients subsequently develop secondary progressive multiple sclerosis, characterized by the progressive and irreversible accumulation of neurological disability (Compston and Coles, 2008; Lassmann *et al.*, 2012; Nylander and Hafler, 2012). Although the pathophysiological processes underlying these two phases of the disease and what determines the transition from one phase to the other are not well understood, recent studies suggest that the progressive phase is linked to a change in the nature of the CNS inflammation that is primarily driven by local innate immune responses (Anderson *et al.*, 2007; Basso *et al.*, 2008; Weiner, 2008; Farez *et al.*, 2009; Mayo *et al.*, 2012, 2014). Current FDA-approved multiple sclerosis therapies act by modulating or suppressing the peripheral immune response and have limited if any effect on progressive forms of multiple sclerosis. Furthermore, many of these therapies are associated with serious side effects (Wingerchuk and Carter, 2014). Thus, identifying novel therapies that address the chronic CNS inflammation associated with progressive forms of multiple sclerosis remains a major unmet need.

Interleukin 10 (IL-10) is a pleiotropic cytokine that has a broad spectrum of anti-inflammatory properties (Moore *et al.*, 2001). Decreased IL-10 levels have been associated with multiple sclerosis severity and with the progressive stage of the disease (van Boxel-Dezaire *et al.*, 1999; Petereit *et al.*, 2003; Soldan *et al.*, 2004) and numerous studies have demonstrated the importance of IL-10 in acute experimental autoimmune encephalomyelitis (EAE) by targeting the peripheral immune response (Moore *et al.*, 2001). Type-1 regulatory T cells (Tr1 cells) have emerged as an important subset of CD4+ T cells that limits excessive inflammatory responses (Roncarolo *et al.*, 2006; Allan *et al.*, 2008). The anti-inflammatory effects of Tr1 cells mainly rely on the secretion of IL-10, which suppresses tissue inflammation and autoimmunity. Accordingly, we and others have shown that treatments that induce Tr1-like cells, such as IL27, or dexamethasone and vitamin D3, were beneficial in the treatment of acute EAE (Barrat *et al.*, 2002; Fitzgerald *et al.*, 2007; Apetoh *et al.*, 2010). Of note, lower levels of vitamin D have been associated with increased disease severity in multiple sclerosis, and a recent study indicated that vitamin D supplementation *in vitro* could partly restore the defective CD46 triggered Tr1 response of patients with relapsing remitting multiple sclerosis (Astier *et al.*, 2007; Kickler *et al.*, 2012; Kleinewietfeld and Hafler, 2014). However, the therapeutic potential of the Tr1/IL-10 axis in progressive disease is unknown, as are its effects on the CNS innate immune system.

A major challenge of immunotherapy is the induction of regulatory T cells, such as Tr1 cells, in a non-toxic and physiological fashion. It is now well-established that stimulation of the mucosal immune system has the unique physiologic property of inducing regulatory T cells (Weiner *et al.*, 2011) and is an attractive, clinically applicable approach that lacks apparent toxicity. We and others have demonstrated that nasal administration of protein antigens or of CD3-specific monoclonal antibody (mAb) is an efficient method for the induction of IL-10 producing $CD4^+$ cells that suppresses inflammatory models of disease (Frenkel *et al.*, 2003; Wu *et al.*, 2008, 2010, 2011; Weiner *et al.*, 2011). Here we report that nasal anti-CD3 induces $IL\text{-}10^+LAP^+$ (latency-associated peptide) Tr1-like T cells that suppress the progressive model of multiple sclerosis in an IL-10-dependent manner by attenuating CNS innate immunity including astrocytes and microglia. These findings identify a new immunological approach for the treatment of progressive forms of multiple sclerosis and potentially other types of chronic CNS inflammation.

Materials and methods

Animals

NOD/ShiLtJ (NOD, non-obese diabetic), C57BL/6 J, and IL-10-GFP knock-in mice (B6.129S6-Il10tm1Flv/J) were from The Jackson Laboratory. Wild-type or IL-10 green fluorescent protein (GFP)-bearing F1 heterozygote mice were generated by breeding NOD mice and wild-type or relevant GFP knock-in C57Bl/6 mice (B6NODF1). All animals were kept in a pathogen-free facility at the Harvard Institutes of Medicine. All experiments were carried out in accordance with guidelines prescribed by the Institutional Animal Care and Use Committee of Harvard Medical School.

EAE induction and treatment

EAE was induced by immunization female mice with myelin oligodendrocyte glycoprotein peptide ($MOG_{35\text{-}55}$) emulsified in complete Freund's adjuvant (Difco Laboratories) at a dose of 100 µg (F1 mice and C57BL/6 J) or 150 µg (NOD mice) per mouse, followed by the administration of pertussis toxin (150 ng per mouse; List biological laboratories, Inc.) on Days 0 and 2 as described (Farez *et al.*, 2009). Clinical signs of EAE were assessed according to the following score: 0, no signs of disease; 1, loss of tone in the tail; 2, hind limb paresis; 3, hind limb paralysis; 4, tetraplegia; 5, moribund. For the induction on nasal tolerance, mice were nasally treated with a daily dose of 1 µg/mouse hamster IgG CD3-specific antibody (clone 145-2C11. BioXCell), or hamster IgG control antibody (BioXCell) dissolved in phosphate-buffered saline (PBS). For some experiments, mice were given 0.5 mg of monoclonal anti-IL-10R blocking antibody (clone 1B1.3A, Bioxcell) or appropriate isotype control (Clone: HRPN, Bioxcell), by intraperitoneal

injection at the onset of the progressive phase, and henceforth every fourth day until experimental end point.

Mouse model of pneumococcal pneumonia

Primary pneumococcal pneumonia was modelled as previously reported (Arredouani *et al.*, 2004; Yang *et al.*, 2015). Pneumonia was induced by intranasal instillation of $\sim 10^5$ colony-forming units (CFU) of *Streptococcus pneumoniae* type 3 into mice under anaesthesia with ketamine (120 mg/kg intraperitoneally) plus xylazine (16 mg/kg intraperitoneally); actual CFU administered were quantitated by CFU assay and used subsequently to calculate per cent clearance. Bronchoalveolar lavage was performed at 24 h of lung inflammation and lung inflammation and bacterial clearance were analysed as previously described (Arredouani *et al.*, 2004; Yang *et al.*, 2015).

Rotarod assay

The rotarod was set to accelerate from a speed of 4 to 40 rotations per min in a 300-s time trial. Each mouse was given an exposure trial to familiarize the animal with the task, and this initial trial was not included for data analysis. Each animal was then given two trials and the times at which mice could no longer successfully manage or remain on the rotarod were averaged and analysed for differences between treatment groups.

MOG_{35-55} tetramer staining

To identify MOG_{35-55} specific T cells, single-cell suspensions from spleen were prepared and stained with MOG_{35-55}-tetramer-PE (MBL) according to manufacturer's instructions. In brief, the cells were stained for 30 min at 4°C, and incubated for additional 30 min with FITC anti-mouse CD3 (145-2C11), APC anti-mouse CD4 (GK1.5) and Brilliant Violet 421™ anti-mouse LAP (TW7-16B4) (all from Biolegend). Cells were analysed using LSR-II FACS analyser in the presence of 7-AAD for the exclusion of non-viable cells. 'Fluorescence minus one' (FMO) controls were used to set the gate.

Near-infrared fluorescence *in vivo* imaging

The IVIS Lumina III In Vivo Imaging System (PerkinElmer) was used to perform *in vivo* near infrared (NIR) imaging. Images were acquired with a 710 nm excitation filter and a Cy5.5 emission filter. Living Image 4.2 software (PerkinElmer) was used for data analysis. Mice were treated nasally with DyLight 755®-conjugated anti-CD3 mAb (clone 145-2C11, Novus Biologicals), and 5 h later the *in vivo* biodistribution of the mAb determined.

Adoptive transfer

To test the *in vivo* regulatory function of the nasally induced T cells we transferred freshly isolated whole CD4+ or CD4+ T cells depleted of LAP^+ cells from anti-CD3 or isotype control-treated NOD mice during the progressive phase of EAE (Day 60) were transferred to a new cohort of NOD mice at the onset of the progressive phase. Each recipient received 4×10^6 T cells intravenously.

Immunohistochemistry

Animals were perfused with PBS, followed by 4% paraformaldehyde in 0.1 M PBS, and tissue was processed and stained as previously described (Mayo *et al.*, 2014). For immunofluorescence staining, sections were stained with GFAP (mouse, 1:300, BD Biosciences), GFP (chicken, 1:500, Abcam), followed by an appropriate fluorophore-conjugated goat secondary antibodies (1:1000; Abcam). Six animals per group were used. Images were taken using a LSM 710 confocal microscope (Carl Zeiss). Paraffin embedded sections were stained with haematoxylin and eosin, Luxol Fast blue for myelin, Bielschowsky silver impregnation for axons, or incubated with primary antibodies against GFAP (rabbit, 1:3000, neomarker), AQP4 (rabbit, 1:250, Sigma), amyloid precursor protein (APP, 1:1000; Milipore), mouse IgG (1:1500, Jackson Research), and fibrin (1:1000, USBIO), followed by biotinylated secondary antibodies (Amersham or Jackson Immuno Research) and bound antibodies, were visualized by diaminobenzidine as chromogen.

In vivo blood–brain barrier permeability

Naïve and isotype control or anti-CD3 treated NOD mice were injected with 0.1 ml of 70 kDa FITC-conjugated dextran (1 mg/ml) into the tail vein, and 600 µl of Evans blue 1%, as previously described (Alvarez *et al.*, 2011) with minor modifications. Mice were anaesthetized 2 h post-injection, perfused with PBS, and Dextran-FITC, and Evans blue extravasation to the spinal cord visualized using a LSM 710 confocal microscope (Carl Zeiss).

Fluorescence-activated cell sorting of astrocytes, microglia and monocytes

Isolated CNS cells were purified by cell sorting using FACSAria I (BD Bioscience) as previously described (Mayo *et al.*, 2014). Microglia were sorted as $CD11b^+$ cells with low CD45 expression and low Ly6C ($CD11b^+ CD45^{low}Ly6C^{low}$), while the inflammatory monocytes were considered as $CD11b^+Ly6C^{high}$ (Prinz *et al.*, 2011). T cells were sorted as $CD3^+CD4^+$ cells. Astrocytes were isolated following the depletion of microglia, monocytes, oligodendrocytes, and lymphocytes [T cells, B cells, and natural killer (NK) cells].

Microarray analysis

RNA was processed, amplified, labelled, and hybridized to Affymetrix GeneChip® MoGene 1.0 ST microarrays (Affymetrix) by the Dana-Farber Cancer Institute Microarray facility. Robust multi-array average (RMA) and quantile normalization were applied for background correction and normalization using the ExpressionFileCreator module of GenePatterns. Differentially expressed genes were identified using the Marker selection module of GeneE (GENE-E version

3.0.224), based on statistical differences in signal-to-noise ratio, following correction for multiple hypotheses testing by computing both the false discovery rate (FDR). Differentially expressed genes were identified as having an FDR < 0.2. Significance Analysis of Microarrays and Gene Set Enrichment Analysis (GSEA) were performed (Subramanian *et al.*, 2005).

nCounter gene expression

Total RNA (50–100 ng) was hybridized with reporter and capture probes for nCounter Gene Expression code sets (Mouse Immunology panel, or a custom made astrocyte-oriented probe set; Mayo *et al.*, 2014), according to manufacturer's instructions analysed by use of the Expander 6.05 platform (Ulitsky *et al.*, 2010).

Quantitative polymerase chain reaction

RNA was extracted with RNeasy® columns (Qiagen), or TRIzol® (Invitrogen), cDNA was prepared and used for quantitative PCR and the results were normalized to *Gapdh* (mice) or *ACTIN* (human). All primers and probes were from Applied Biosystems, *Aqp4* (Mm00802131_m1), *Mmp3* (Mm00440295_m1), *Mmp9* (Mm00442991_m1), *Ccl5* (Mm01302427_m1), *Cd40* (Mm00441891_m1), *Csf2* (Mm01290062_m1), *Cxcl10* (Mm00445235_m1), *Foxp3* (Mm00475162_m1), *Gapdh* (Mm00484668_m1), *Gfap* (Mm01253033_m1), *H2-Aa* (Mm00439211_m1), *Ifng* (Mm01168134_m1), *Il10* (Mm00439614_m1), *Il17a* (Mm00439618_m1), *Il1b* (Mm00434228_m1), *Il14* (Mm00445259_m1), *Il6* (Mm00446190_m1), *Nos2* (Mm00440502_m1), *Spp1* (Mm00436767_m1), *Tbx21* (Mm00450960_m1), *Tgfb1* (Mm01178820_m1), *Tlr2* (Mm00442346_m1), *Tnf* (Mm00443260_g1), *Vegfa* (Mm01281449_m1), *Irf7* (Mm00516793_g1), *Gata3* (Mm00484683_m1), *ACTB* (Hs01872448_s1), *IL10RA* (Hs00155485_m1).

T cell proliferation and cytokine measurement

Splenocytes and lymph node cells were cultured for 72 h in the presence of anti-CD3 mAb or MOG_{35-55} peptide, and cell proliferation and cytokine production was determined as previously described (Mayo *et al.*, 2014).

For intracellular cytokine staining, cells were stimulated for 6 h with PMA (phorbol 12-myristate 13-acetate; 50 ng/ml; Sigma), ionomycin (1 μg/ml; Sigma) and monensin (GolgiStop; 1 ml/ml; BD Biosciences). After staining of surface markers, cells were fixed and made permeable according to the manufacturer's instructions BD Cytofix/Cytoperm™ Kit (BD Biosciences), or Foxp3 Fixation/Permeabilization (Ebioscience).

T cell suppression assay

$CD4^+LAP^+$ T cells were sorted from anti-CD3 or isotype control-treated NOD mice, 60 days after EAE induction (Fig. 1). Cells were cultured at a 1:1 ratio with syngeneic naive responder $CD4^+$ T cells ($CD4^+CD62L^{high}CD44^{low}$) previously stained with CellTrace™ Violet according to the manufacturer's recommendation (CellTrace™ Violet proliferation kit; Invitrogen). Cells were stimulated with 1 μg/ml of soluble anti-CD3 in the presence of mitomycin-treated antigen-presenting cells. Proliferation was assessed 48 h later by flow cytometry based on the dilution of the CellTrace™ Violet dye on responder cells. In some experiments, monoclonal anti-IL-10R blocking antibody (clone 1B1.3A, Bioxcell) or appropriate isotype control (clone: HRPN, Bioxcell) were added (50 μg/ml) directly to the co-culture.

T cell differentiation *in vitro*

Naive $CD4^+CD62L^{high}$ $CD44^{low}GFP^{neg}$ T cells were stimulated for 60 h using plate-bound antibody to CD3 (2 μg/ml) (145-2C11, Biolegend) and soluble antibody to CD28 (2 μg/ml) (PV-1, BioXcell) in the presence of recombinant cytokines. T cells were polarized with recombinant TGF-β1 (3 ng/ml, R&D) for $FOXP3^+$ Treg, recombinant IL27 (30 ng/ml, ebioscience) or recombinant IL27 and TGF-β1 for Tr1 cells, and Tho were maintained with recombinant mouse IL2 (10 ng/ml).

Mouse primary microglia

Mouse primary microglia were prepared as described (Saura *et al.*, 2003; Mayo *et al.*, 2014) with minor modifications. Microglia purity were >98%, as determined by staining with fluorescein-conjugated *Griffonia simplicifolia* isolectin B4 (IB4) (Vector Laboratories) or PE-conjugated CD11b antibody (data not shown).

Mouse primary astrocytes

Mixed glia were prepared as described (Saura *et al.*, 2003; Mayo *et al.*, 2014), and cultured until confluent (Day 7–10). The cells were then incubated with 0.02 mg/ml of clodronate encapsulated liposomes (Clodrosome) (Encapsula NanoSciences LLC) for 2–3 days, washed, and the astrocyte monolayer separated using the mild trypsinization procedure, and plated. Cells were >99% astrocytes, as determined by staining with GFAP or GLAST, with <1% contamination of $CD11b^+$ microglia cells (data not shown).

In vivo astrocyte-specific knock-down with short hairpin RNA lentivirus

pLenti-GFAP-EGFP-mir30-short hairpin (sh)RNA harbouring shRNA sequences against *Il10ra*, or a non-targeting shRNA were cloned using the pLenti-pGFAP-EGFP-mir30-shRNA vector (Yan *et al.*, 2012) or the pLenti-pCD11b-EGFP-mir30-shRNA (Ding *et al.*, 2015) as a backbone, by replacing the shRNA for Act1 with the abovementioned *in vitro* validated shRNA sequences (*Il10ra* :5'- *ccgg*CCGCTTGGAATCCCGAATTAA*ctcgag*TTAATTCGGGATTCCAAGCGG*ttttt*g-3') and a non-targeting shRNA. Lentivirus particles were then generated as described (Mayo *et al.*, 2014).

NOD EAE mice, 35 days after immunization (progressive phase), were anaesthetized with isoflurane and placed in a Kopf Stereotaxic Alignment System. Using a Hamilton syringe, 10^7 IU/mouse of shIL10ra, or shControl (non-targeting) virus were injected 0.5 mm posterior to the bregma, ±1.0 mm lateral to it and 2.2 mm below the skull surface.

Monocyte migration assay

Splenic Ly6Chigh monocytes were freshly sorted ($CD11b^+F4\text{-}80^+SSC^{low}Ly6C^{high}$), and their ability to migrate towards CCL2 (50 ng/ml, peprotech), astrocyte-conditioned media, or vehicle control (PBS), was determined as previously described (Mayo *et al.*, 2014).

Multiple sclerosis tissue

Brain tissue was obtained from patients with multiple sclerosis with clinically diagnosed and neuropathologically confirmed multiple sclerosis, or healthy controls were immediately frozen in liquid nitrogen. White matter multiple sclerosis tissue samples were selected as previously described (Alvarez *et al.*, 2011). All patients and controls, or their next of kin, had given informed consent for autopsy and use of their brain tissue for research purposes. Ethic approval was given prior to autopsy (CHUM ethic approval: SL05.022 and SL05.023 and BH07.001).

Statistical analysis

Statistical data analysis was performed with Prism software version 6.0 g (GraphPad Software). For comparisons of two groups, two-tailed Student's *t*-test was used. Comparisons of multiple groups were made using one-way or 2-way ANOVA, as described in the figure legends. Analysis of EAE clinical scores was corrected for repeated measures, and also subjected to linear regression analysis (95% confidence interval) for the analysis of the treatment effect on disease progression. Data represent mean ± standard error of the mean (SEM). $P < 0.05$ was considered significant.

Results

Nasal anti-CD3 monoclonal antibody ameliorates disease in a progressive model of EAE

To study the therapeutic effect of nasal anti-CD3 in a model of progressive CNS inflammation, we investigated the course of EAE in NOD mice that develop a form of EAE that resembles progressive multiple sclerosis (Basso *et al.*, 2008; Farez *et al.*, 2009; Mayo *et al.*, 2014). In this model, NOD mice immunized with a myelin oligodendrocyte glycoprotein peptide ($MOG_{35\text{-}55}$) develop a self-limited acute neurological syndrome (acute phase) followed by a phase of irreversible progressive neurological impairment (progressive phase). We immunized NOD mice with $MOG_{35\text{-}55}$, and initiated treatment at the onset of the progressive phase (Day 30 after immunization). We found that daily nasal administration of CD3-specific mAb (1 µg/mice) suppressed disease progression in terms of clinical score, motor performance, demyelination, axonal integrity and lesion load as compared to mice treated with an isotype control antibody, at the experimental endpoint (Day 70) (Fig. 1A–G). Anti-CD3 mAb administration also restored blood–brain barrier integrity as demonstrated by reduced extravasation of endogenous fibrin and antibody to the spinal cord (Fig. 1H). To further investigate this finding, we administered the Evans blue tracer dye intraperitoneally and FITC-conjugated dextran intravenously to measure ongoing blood–brain barrier integrity, as described (Alvarez *et al.*, 2011). We found no extravasation of Evans blue or FITC-conjugated dextran (Figs. 1I and J) demonstrating that nasal anti-CD3 administration limits blood–brain barrier disruption resulting from the inflammatory response. Similar results were obtained when we administered nasal anti-CD3 mAb after progression was well established (Day 45 after immunization), which may represent a more clinically relevant therapeutic time for treatment, and found rapid reversal of clinical progression (Fig. 1K). To determine whether nasal anti-CD3 reached the CNS we analysed the distribution of near-infrared fluorescence labelled anti-CD3 mAb administrated nasally using an *in vivo* imaging system and found that the antibody accumulated in the cervical lymph nodes, but was not detected in the CNS (Supplementary Fig. 1A). Of note, neither microglia nor astrocytes express the CD3ε chain, and they are not stained by anti-CD3 mAb (Supplementary Fig. 1B and C). Nasal anti-CD3 mAb did not impair the ability to clear bacterial infection in the lung (Supplementary Fig. 1D–F). We then studied the effects of nasal anti-CD3 mAb in acute EAE and similarly found that daily administration ameliorated disease progression in the later stages of EAE; it did not affect disease onset (Supplementary Fig. 2A). Taken together, these data demonstrate an ameliorating effect of nasal anti-CD3 mAb administration on progressive stages of EAE.

Nasal anti-CD3 monoclonal antibody induces an $IL\text{-}10^+LAP^+$ T cell that attenuates progressive EAE in an IL-10-dependent manner

We have previously shown that regulatory T cells induced by the nasal administration of anti- CD3 express IL-10 (Wu *et al.*, 2008, 2009, 2010, 2011). Thus we asked whether nasal anti-CD3 mAb induces IL-10 producing T cells during the progressive phase of EAE in the NOD model. In the spleen, we found increased IL-10 secretion following both MOG and anti-CD3 agonist mAb restimulation, and increased IL-10 expression by the T cells after stimulation with PMA/ionomycin (Fig. 2A and B). Of note, we did not observe upregulation of signature cytokines or transcription factors associated with other $CD4^+$ T-cell subsets known to secrete IL-10 including $FOXP3^+$ Tregs (regulatory T cells) and Th2 cells (Supplementary Fig. 2B and C, and Fig. 2G). We did find that nasal anti-CD3 mAb induced the expression of latency-associated peptide (LAP) (Supplementary Fig. 2D and E), a plasma membrane protein associated with regulatory T cell lineages, and that many of the induced $IL\text{-}10^+$ T cells (57.4 ± 2.7%) were

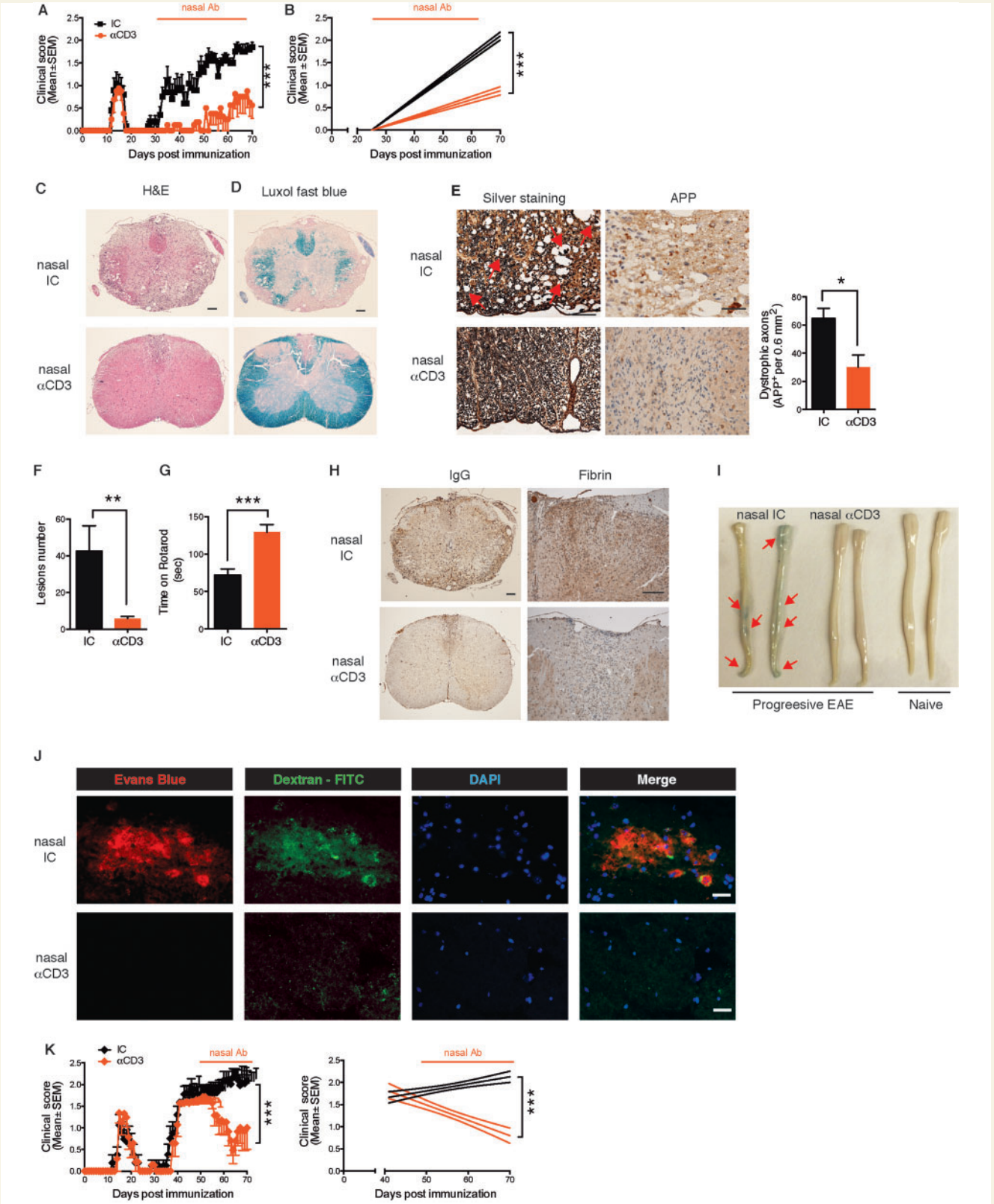

Figure 1 Nasal anti-CD3 ameliorates disease in a progressive model of EAE. (**A** and **B**) Clinical scores of EAE in NOD mice treated nasally with CD3 specific or isotype control mAbs, administered daily (1 μg/mouse) from Day 30 after EAE induction (progressive phase) for the duration of the experiment. Representative data of eight independent experiments with $n = 8$ mice/group (mean and SEM), statistical analysis by two-way ANOVA and linear regression. (**C–J**) At the experimental endpoint (Day 70) mice Rotarod performance was evaluated (**G**), and (**I–J**) histopathology analysis of lumbar spinal cord serial sections from EAE NOD mice treated with anti-CD3 or isotype control as in **A** was performed. Sections were stained with haematoxylin and eosin (H&E), Luxol Fast blue stain or Bielschowsky's silver impregnation for analysis of

(continued)

LAP$^+$ (Fig. 2C). Notably, we observed that many of the LAP$^+$ T cells were MOG-specific (65.1 ± 4.9%) (Fig. 2D). We found an increase in CNS T cells in nasal anti-CD3 mAb treated mice (Fig. 2E and F), and these T cells had increased IL-10 expression (Fig. 2G and H).

We then asked whether the protective effects of nasal anti-CD3 mAb were linked to LAP$^+$ and IL-10$^+$ T cells. To address this point, we initially analysed the suppressive function of anti-CD3 mAb induced CD4$^+$LAP$^+$ T cells *in vitro*. We co-cultured CFSE-labelled naïve T cells (responder T cells) with CD4$^+$LAP$^+$ T cells isolated from anti-CD3 mAb-treated NOD mice during the progressive phase of EAE (Day 60) (Fig. 2I). We found that the anti-CD3 mAb-induced T cells suppressed the responder T cell proliferation. We then performed adoptive transfer experiments in which isolated CD4$^+$ T cells from anti-CD3 mAb or isotype control-treated NOD mice during the progressive phase of EAE (Day 60) were transferred to a new cohort of NOD mice at the onset of the progressive phase (Fig. 2J). We found that the anti-CD3 mAb induced T cells attenuated the progressive phase of NOD EAE to the same extent as anti CD3 mAb treated mice. Moreover, the effect was dependent on LAP$^+$ T cells, as protection was reversed by depletion of LAP$^+$ T cells prior to cell transfer (Fig. 2J). Of note, the beneficial effect of adoptive transfer of splenic CD4$^+$ T cells from anti-CD3 mAb-treated mice declines after a week.

Next, we investigated the role of IL-10 on the therapeutic effect of nasal anti-CD3 mAb using anti-IL-10 receptor (IL-10R) blocking antibodies. We found that the suppression by anti-CD3 mAb induced T cells *in vitro* was reversed when IL-10 signalling was blocked (Fig. 2K), and moreover that the therapeutic effect of the nasal anti-CD3 was also abrogated when IL-10 signalling was blocked (Fig. 2L). Of note, blocking IL-10 signalling did not worsen the clinical course of the disease in the isotype control group, suggesting that during the normal course of EAE the low/basal expression of IL-10 lacks significant biological relevance to the disease progression.

We also found that *IL10RA*, which encodes for the ligand-binding subunit of the IL-10 receptor (Moore *et al.*, 2001) is significantly upregulated during chronic CNS inflammation, both in NOD mice following EAE induction (Supplementary Fig. 3A), and in multiple sclerosis lesions (Supplementary Fig. 3B), suggesting that treatments that target IL-10 may be of benefit. Of note, we were not able to detect IL-10 in the brain material of our cohort of patients with multiple sclerosis. Consistent with this, using proteomic and transcriptomic analysis, Steinman's group also did not identify IL-10 expression in the CNS of patients with multiple sclerosis (Lock *et al.*, 2002; Han *et al.*, 2008).

Taken together, these data demonstrate that nasal anti-CD3 mAb induces active regulation of progressive EAE, through a mechanism mediated by IL-10$^+$LAP$^+$ CD4$^+$ T cells.

Nasal anti-CD3 induces IL-10$^+$ Tr1-like cells

IL-10-secreting regulatory T cells could represent Tr1 cells, FOXP3 Treg cells or be generated from a different lineage of T cells that have undergone chronic stimulation, resulting in the disappearance of effector T cell cytokines but the maintenance of IL-10 (exhausted T cells). To characterize the anti-CD3 mAb induced IL-10 secreting Tregs, we performed microarrays on these cells and compared them to naïve T cells, FOXP3$^+$ Tregs and IL27-induced Tr1 cells. To perform this experiment, we used mice that express GFP on the IL-10 promoter, which provided a way to sort IL-10$^+$ T cells *ex vivo*. We generated F1 hybrid mice derived by breeding NOD and C57BL/6IL-10:GFP (B6NODF1IL-10:GFP). We have previously shown that NOD × C57BL/6 mice develop a chronic progressive form of EAE (Mayo *et al.*, 2014). We first established that nasal anti-CD3 attenuates the progressive phase of EAE in B6NODF1IL-10:GFP mice (Fig. 3A). We then isolated CD3$^+$CD4$^+$GFP (IL-10)$^+$ cells from the cervical lymph nodes and spleen of anti-CD3 mAb treated B6NODF1IL-10:GFP mice during the progressive phase of EAE (Fig. 3B) and compared their transcriptional profile to naïve (CD3$^+$CD4$^+$CD62L^{high}CD44^{low}) T cells using a microarray. We assessed the reproducibility of our data and conservation across biological replicates by calculating the correlations across all samples. We found a strong correlation among cell type replicates (Pearson correlation coefficient = 0.9828–0.9914), lower correlations between the naïve and anti-CD3 mAb induced cell types, and a strong correlation between anti-CD3 mAb induced cells recovered from the cervical lymph nodes or spleen (Supplementary Fig. 4A and Supplementary Table 1). Analysis of the cell

Figure 1 Continued

mononuclear cell infiltration and vacuoles indicating oedema, demyelination or axonal loss (axonal injury with spheroids is identified by red arrows), respectively. Representative data of two independent experiments with $n = 6$ mice/group, statistical analysis by Student's *t*-test (**E–G**) Quantification of dystrophic axons as determined by amyloid precursor protein (APP) staining and lesions load, respectively. Representative data of two independent experiments with $n = 6$ mice/group, statistical analysis by Student's *t*-test. (**H–J**) Blood–brain barrier permeability. (**H**) Extravasation of endogenous fibrin and antibodies (IgG), and (**J**) exogenous tracer dye Evans Blue or FITC-conjugated dextran to the spinal cord. Representative data of two independent experiments with $n = 5$ mice/group. (**K**) Clinical scores of EAE in NOD mice treated nasally with CD3 specific or isotype control mAbs from Day 45 after EAE induction. Representative data of two independent experiments with $n = 8$ mice/group (mean and SEM), statistical analysis by two-way ANOVA. Scale bar = 100 μm for low power magnification (**C** and **H**), and 50 μm (**C–E** and **H**) or 20 μm (**J**) for higher magnification. $^*P < 0.05$, $^{**}P < 0.01$, $^{***}P < 0.001$, n.s. = not significant.

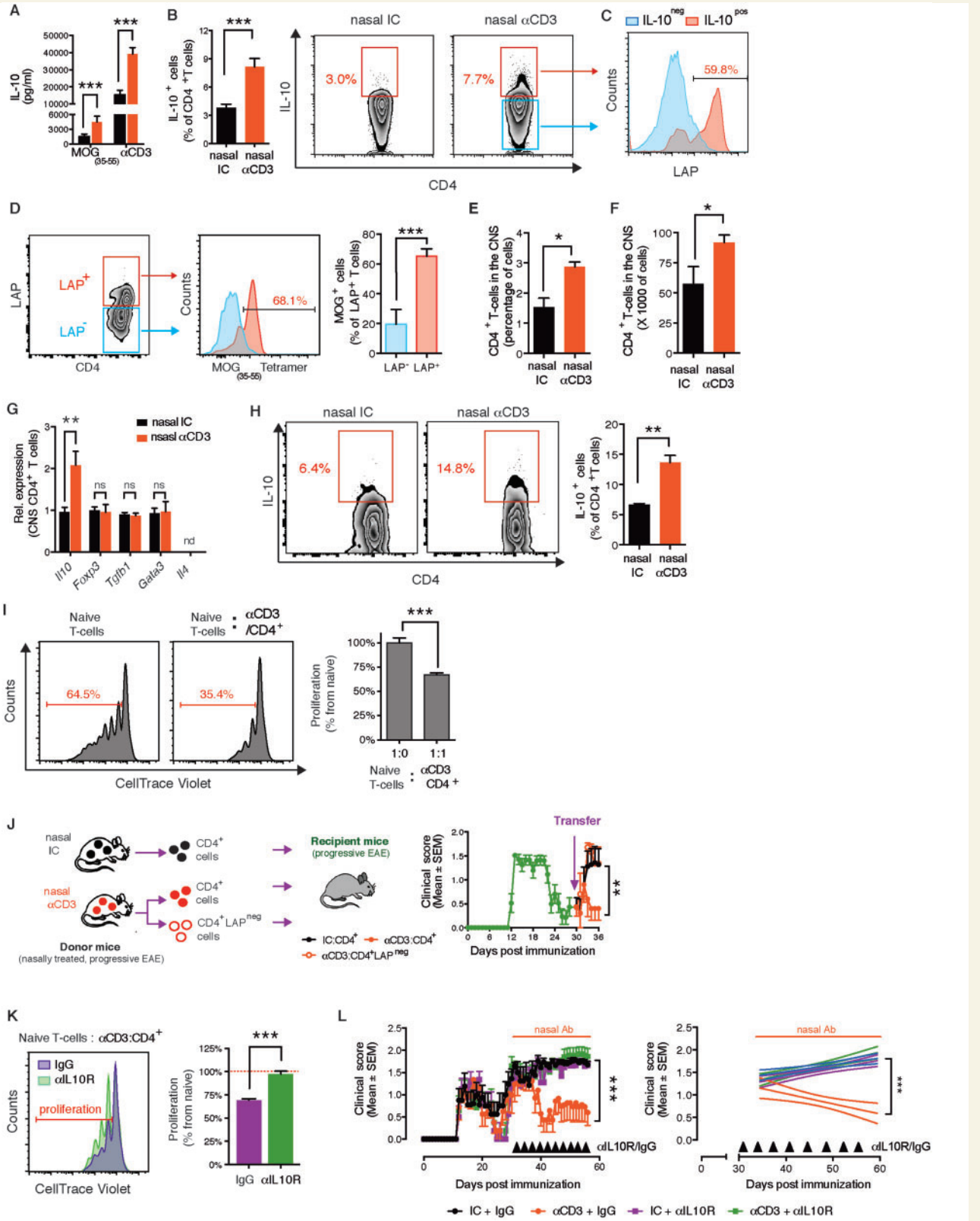

Figure 2 Nasal anti-CD3 induces an IL-10 + LAP + T- cell that attenuates progressive EAE in an IL-10 dependent manner. (**A–I**) NOD mice treated nasally with CD3 specific or isotype control mAbs following EAE induction as in (Fig. 1A). IL-10 secretion by splenic T cell in response to $MOG_{35–55}$ (20 μg/ml) or anti-CD3 mAbs (0.2 μg/ml) stimulation was determined by enzyme-linked immunosorbent assay (**A**), and IL-10 and LAP expression by splenic $CD4^+$ T cells was examined by fluorescence-activated cell sorting (FACS) (**B** and **C**). Data are representative of four independent experiments with $n = 6$ mice/group (mean and SEM). Statistical analysis by Student's *t*-test. (**D**) Proportion of MOG-specific T cells within LAP^+ and LAP^- splenic T cells in NOD EAE mice treated with nasal anti-CD3. Data are representative of two independent

(continued)

transcriptomes revealed that 747 genes were differentially expressed (FDR < 0.2) in anti-CD3 mAb induced IL-10$^+$ T cells versus naïve T cells (Fig. 3C). These genes were associated with multiple cellular functions including cell cycle, cytokine and chemokine activity, ATP binding and the regulation of the immune response (Fig. 3D). The strongest functional enrichment was associated with positive regulation of cell proliferation. Indeed, most of IL-10 secreting T cells isolated from anti-CD3 treated NOD were proliferating as measured by high expression of Ki-67 (57.3 ± 2.09%) or by measuring the proliferation of *ex vivo* restimulated CFSE-labelled cells (90.6 ± 0.01%) (Fig. 3E and F, respectively). Thus, these results suggest that nasal anti-CD3 mAb induced T cells are differentiated T cells as opposed to exhausted T cells.

We then compared the transcriptional profiles of *in vitro*-defined T cell linages to nasal anti-CD3 mAb induced T cells. For these comparisons, we investigated Th0 cells, FOXP3$^+$ Tregs, and Tr1 cells (differentiated with IL27 or TGFβ$^+$IL27) (Apetoh *et al.*, 2010) (Supplementary Fig. 4B). Evaluation of the cell transcriptomes revealed strong correlations among cell type replicates and lower correlations across differing cell types (Supplementary Fig. 4C). We found that 514 genes were differentially regulated by Tr1 cells (FDR < 0.2), and that 255 genes were differentially regulated (FDR < 0.2) by Tregs, as compared to Th0 cells (Supplementary Fig. 4D and E, and Supplementary Tables 2 and 3, respectively).

To investigate the relationship between anti-CD3 induced IL-10$^+$ cells and other T cell types we used principal component analysis (PCA) (Fig. 3F and G, respectively). PC1 was associated with the variance between the *in vivo* and *in vitro* generated datasets, whereas PC2 was associated with the variance between cell linage and function (Fig. 3F). We thus focused our analysis on PC2 and found that nasal anti-CD3-induced T cells are more closely associated with *in vitro* differentiated Tr1 cells than FOXP3 Tregs and that this is primarily driven by genes associated with known Tr1-linked genes such as *IL10*, *IL21* and *MAF* (previously known as c-MAF) (Apetoh *et al.*, 2010) (Fig. 3G). To determine the degree of similarity between nasal anti-CD3 induced T cells and *in vitro* induced Tr1 cells, we used Gene Set Enrichment Analysis (GSEA) (Subramanian *et al.*, 2005) (Fig. 3H). We compared the upregulated genes from the Tr1 signature (349 genes) to those of the anti-CD3 mAb *in vivo* induced T cells, and found a strong enrichment for Tr1 signature genes (FDR q-value = 0.03) (Subramanian *et al.*, 2005). These results demonstrate that nasal anti-CD3-induced T cells are Tr1-like. In agreement with these findings, adoptive transfer of *in vitro* differentiated IL-10$^+$ Tr1 cells at the onset of the progressive phase of B6NODF1 EAE, resulted in suppression of EAE, mirroring the therapeutic effects of the IL-10$^+$LAP$^+$ T cells, induced by the nasal anti-CD3 administration (Fig. 3I).

Taken together, these results demonstrate that IL-10-secreting T cells, induced by nasal anti-CD3 mAb administration, resemble Tr1 cells.

Nasal anti-CD3 monoclonal antibody attenuates the adaptive T cell response

To evaluate the effects of nasal anti-CD3 mAb on the peripheral adaptive immune response, we measured the response of splenocytes isolated from isotype control or anti-CD3 mAb treated mice to restimulation with MOG_{35-55} or anti-CD3 mAb. We found that nasal anti-CD3 mAb compromised the peripheral adaptive response by reducing the proliferative response to *ex vivo* stimulation (Fig. 4A and B). Furthermore, the frequency of IL17$^+$ T cells in the periphery was reduced following nasal anti-CD3 mAb treatment (Fig. 4C). Consistent with this, we found a reduction in the expression levels of IL17 encoding gene and the transcription factor RORgt (*Il17a* and *Rorc*) in T cells sorted from the CNS of nasal anti-CD3 mAb-treated mice (Fig. 4D). Of note, we did not observe changes in the expression of granulocyte-macrophage colony-stimulating factor (GM-CSF; associated with pathogenic T cells) or T-bet and IFNγ (associated with the Th1 lineage) (Fig. 4D and Supplementary Fig. 1F and G).

Thus, nasal anti-CD3 mAb both reduces Th17 polarization and induces IL-10$^+$-Tr1 like cells, which is consistent with a report that Tr1 cells regulate Th17 polarization via

Figure 2 Continued

experiments with $n = 5$ mice/group (mean and SEM). Statistical analysis by Student's *t*-test. Relative and absolute numbers of CNS-infiltrating CD4$^+$ T cells was determined by FACS (**E** and **F**, respectively). (**G**) Quantitative PCR analysis of the expression of *Il10*, *Foxp3*, *Tgfb1*, *Gata3*, *and Il4* mRNA of CD4$^+$ T cells isolated from the CNS; expression is presented relative to *Gapdh*. (**H**) IL-10 expression by CNS-infiltrating CD4$^+$ T cells was examined by FACS (**I** and **K**) FACS-sorted CD4$^+$ T cells from nasal anti-CD3 treated NOD EAE mice (Day 60) were used in a standard suppression assay with naive CD4$^+$ responder T cells at a ratio of 1:1 (**I**). To test the role of IL-10 in *in vitro* suppression, isotype control (IC) or anti-IL-10 R (50 μg/ml) blocking antibodies were added to co-cultures (**K**). Representative data of two independent experiments with $n = 4$ mice/group, statistical analysis by Student's *t*-test. (**J**) Clinical scores of EAE in NOD mice following adoptive transfer (4×10^6 cells/mouse) of splenic CD4$^+$, or CD4$^+$LAP^{neg} T cells sorted from chronic NOD EAE mice (Day 60) that were treated with anti-CD3 as in Fig. 1A. Representative data of two independent experiments with $n = 5$ mice/group (**L**) Clinical scores of EAE in NOD mice. At the onset of the chronic phase of EAE mice were treated daily with nasal CD3 specific or isotype control mAbs, and were intraperitoneally injected every fourth day (black arrows) with anti-IL-10 receptor blocking mAbs (αIL-10 R) or appropriate control (IgG) (0.5 mg/mouse). Representative data of two independent experiments with $n = 8$ mice/group. $^*P < 0.05$, $^{**}P < 0.01$, $^{***}P < 0.001$, n.s. = not significant; n.d. = not detected.

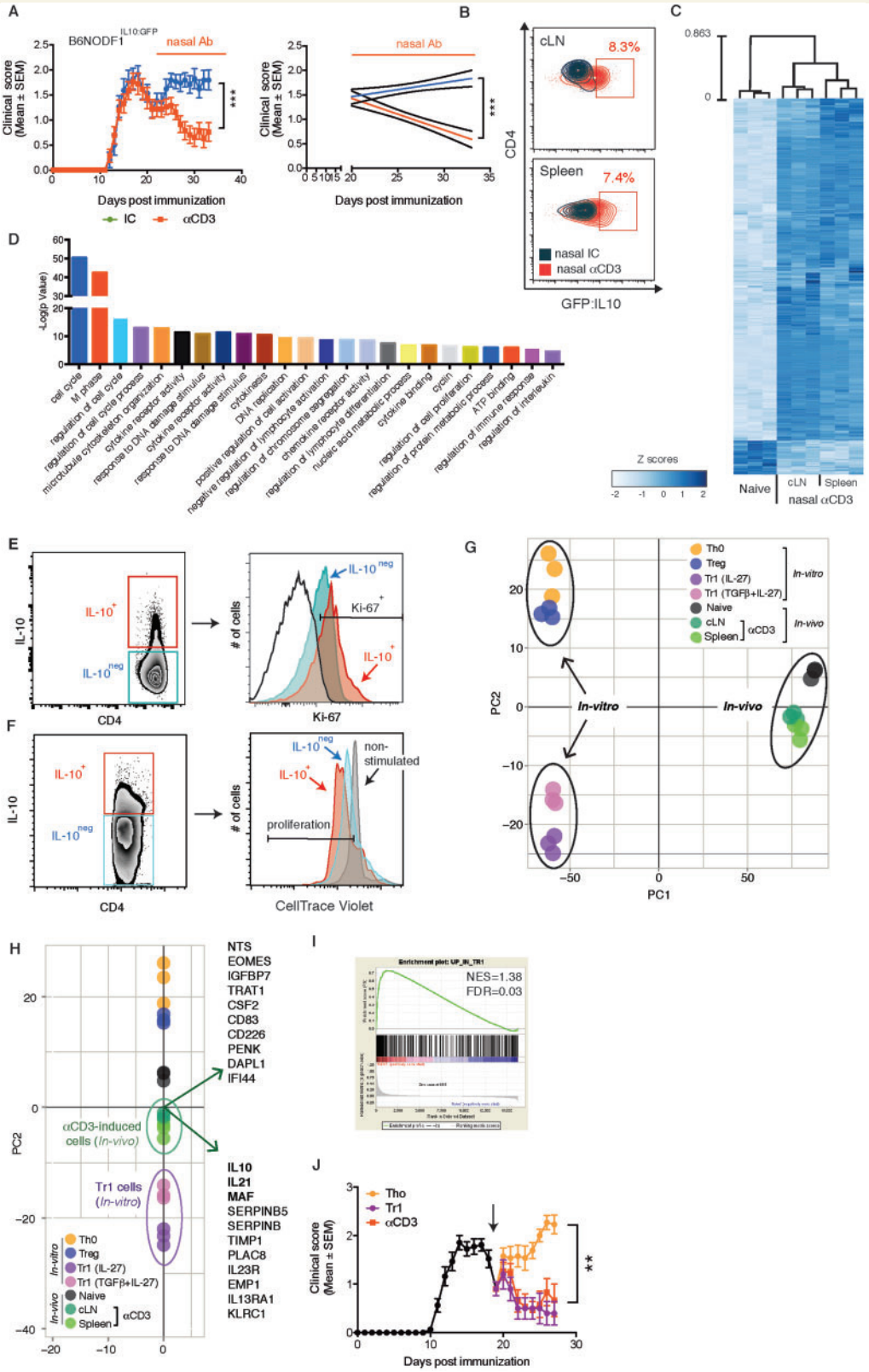

Figure 3 Nasal anti-CD3 induces IL-10$^+$ Tr1-like cells. (**A–H**) EAE was induced in IL-10:GFP F1 hybrid mice (B6NODF1IL-10:GFP) and mice were treated nasally with CD3 specific or isotype control mAbs as in Fig. 1A. (**A**) Nasal anti-CD3 attenuates the of progressive phase of EAE in the B6NODF1IL-10:GFP mice. Data are representative of two independent experiments with $n = 8$ mice/group (means and SEM). (**B**) GFP (IL-10) expression by CD4$^+$ T cells in the spleen and cervical lymph nodes (cLN) was examined by flow cytometry. (**C**) Heat map depicting the differential mRNA expression profiles in naïve CD4$^+$ or CD4$^+$ GFP/IL-10$^+$ T cells isolated from the spleen or cLNs of B6NODF1IL-10:GFP mice during the progressive phase of EAE following nasal treatment, as detected by microarray data analysis. (**D**) Functional enrichment analysis of the

(continued)

IL-10 dependent signalling (Huber *et al.*, 2011). Given that Th17 responses are increased in subjects with progressive multiple sclerosis (Huber *et al.*, 2014) regulation of Th17 levels by nasal anti-CD3 mAb may contribute to its therapeutic potential for the treatment of progressive multiple sclerosis.

Nasal anti-CD3 monoclonal antibody suppresses astrocyte activation in an IL-10-dependent manner

Astrocytes play an important role in the response of the CNS to inflammation including maintenance of blood–brain barrier integrity, regulation of the influx of T cells and monocytes from the periphery to the CNS and modulation of microglia and oligodendrocytes within the CNS (Myer *et al.*, 2006; Mayo *et al.*, 2012). In addition, we have identified a crucial role for astrocytes during CNS inflammation in the progressive phase of NOD EAE (Farez *et al.*, 2009; Mayo *et al.*, 2014). Thus, we investigated the effects of nasal anti-CD3 mAb on astrocytes in the progressive NOD EAE model.

We isolated astrocytes from naïve mice and from isotype control or nasal anti-CD3-treated mice on Day 70 of progressive EAE and analysed their transcriptome by Nanostring nCounter arrays using a custom-made astrocyte probe set (Mayo *et al.*, 2014) shown in (Supplementary Table 4). We identified genes that were upregulated during EAE and downregulated by nasal anti-CD3 mAb, and genes downregulated during EAE and upregulated by nasal anti-CD3 (Fig. 5A). We then validated selected genes by quantitative PCR that are known to play an important role in CNS inflammation (Fig. 5B). We found downregulation of *Ccl2*, which is involved in recruitment of monocytes to the CNS (Izikson *et al.*, 2000; Mildner *et al.*, 2009) and of *Ccl5*, which is important for recruitment of peripheral immune cells to the CNS. IL6 (*Il6*) and toll-like receptor 2 (*Tlr2*) were downregulated, both of which are pro-inflammatory genes in the CNS (Farez *et al.*, 2009; Miranda-Hernandez and Baxter, 2013). Of note, we found upregulation of the water channel aquaporin 4 (*Aqp4*), which has recently been associated with astrocyte regulation of diverse processes ranging from CSF circulation, waste clearance, neuroinflammation, cell migration, and Ca^{2+} signalling (Nagelhus and Ottersen, 2013). Restoration of AQP4 following nasal anti-CD3 was also observed by immunohistochemistry (Fig. 5C). Of note, loss of AQP4 staining in chronic EAE was not secondary to loss of astrocytes, as shown by preserved GFAP staining (Fig. 5C).

As astrocytes regulate axonal myelination (Watkins *et al.*, 2008; Mayo *et al.*, 2012) we also studied the expression levels of genes ($n = 29$) associated with demyelination at the chronic phase of NOD EAE (Day 70), as measured by the astrocyte Nanostring code set (Supplementary Table 5). In agreement with the demyelination and axonal damage shown in Fig. 1C–E, we detected upregulation of astrocytic genes associated with demyelination in progressive NOD EAE that was reduced following nasal anti-CD3 mAb administration (Supplementary Fig. 5). We present a composite statistical analysis of these results in Fig. 5D. We also focused on the effect of nasal anti-CD3 mAb on the role of astrocytes on regulating blood–brain barrier integrity (Argaw *et al.*, 2012) and consistent with what we show in Fig. 1H–J, we found upregulation of astrocytic genes associated with blood–brain barrier degradation (*Vegfa*, *Mmp3*, *Mmp9*) that was reversed by nasal anti-CD3 mAb (Fig. 5E). Taken together, these data demonstrate that nasal anti-CD3 mAb attenuates astrocyte activation during progressive EAE.

To investigate whether IL-10 acts directly on murine astrocytes to regulate their function, we investigated the effect of IL-10 on primary astrocyte cultures. We found that IL-10 suppressed the expression of *Ccl2*, *Ccl5*, *Csf2*, *Nos2*, *Mmp3* and *Mmp9* following stimulation with IL1β (Fig. 5F). Two of these are primary molecules used by astrocytes to modulate to the CNS immune microenvironment: CCL2, which regulates Ly6Chi inflammatory monocytes recruitment to the CNS (Kim *et al.*, 2014; Mayo *et al.*, 2014) and GM-CSF (*Csf2*), which induces a pro-inflammatory phenotype in mononuclear phagocytes (Mayo *et al.*, 2014).

To investigate the role of the IL-10-astrocyte axis on the *in vivo* effect of nasal anti-CD3 mAb, we used a strategy in which we knocked-down the expression of the ligand-binding subunit of the IL-10 receptor (*Il10ra*) expression in astrocytes. We used a lentivirus-based system optimized for astrocyte-specific knock-down *in vivo* (Yan *et al.*, 2012; Mayo *et al.*, 2014), in which the expression of the

Figure 3 Continued

differentially expressed genes. Flow cytometry analysis of IL-10 and Ki-67 expression by CD4+ T cells isolated from anti-CD3 treated NOD mice (**E**), and their IL-10 expression following CFSE-labelling and *ex vivo* restimulation (**F**). Data are representative of two independent experiments with $n = 5$ mice/group. (**G** and **H**) PCA of differentially regulated genes of *in vivo* and *in vitro* sorted regulatory T cell listed in (Supplementary Tables 1 and 2); circles indicate grouping. Biplot in **H** displays the top 20 genes with the maximal variances that drive the population functional segregation (PC2). (**I**) Gene set enrichment analysis (GSEA) of the upregulated genes *in vitro* differentiated Tr1 cells, and the *in vivo* induced IL-10$^+$ T cells. Normalized enrichment score (NES) of 1.389 and FDR q-value (FDR) of 0.0382. (**J**) Clinical scores of EAE in wild-type F1 hybrid mice (B6NODF1) mice. At the onset of the chronic phase mice were treated with anti-CD3 or subjected to adoptive transfer of sorted *in vitro* differentiated Tr1 or Tho cells. Representative data of two independent experiments with $n = 7$ mice/group (means and SEM). Statistical analysis of EAE clinical score in (**A** and **J**) by two-way ANOVA. $^{**}P < 0.01$, $^{***}P < 0.001$.

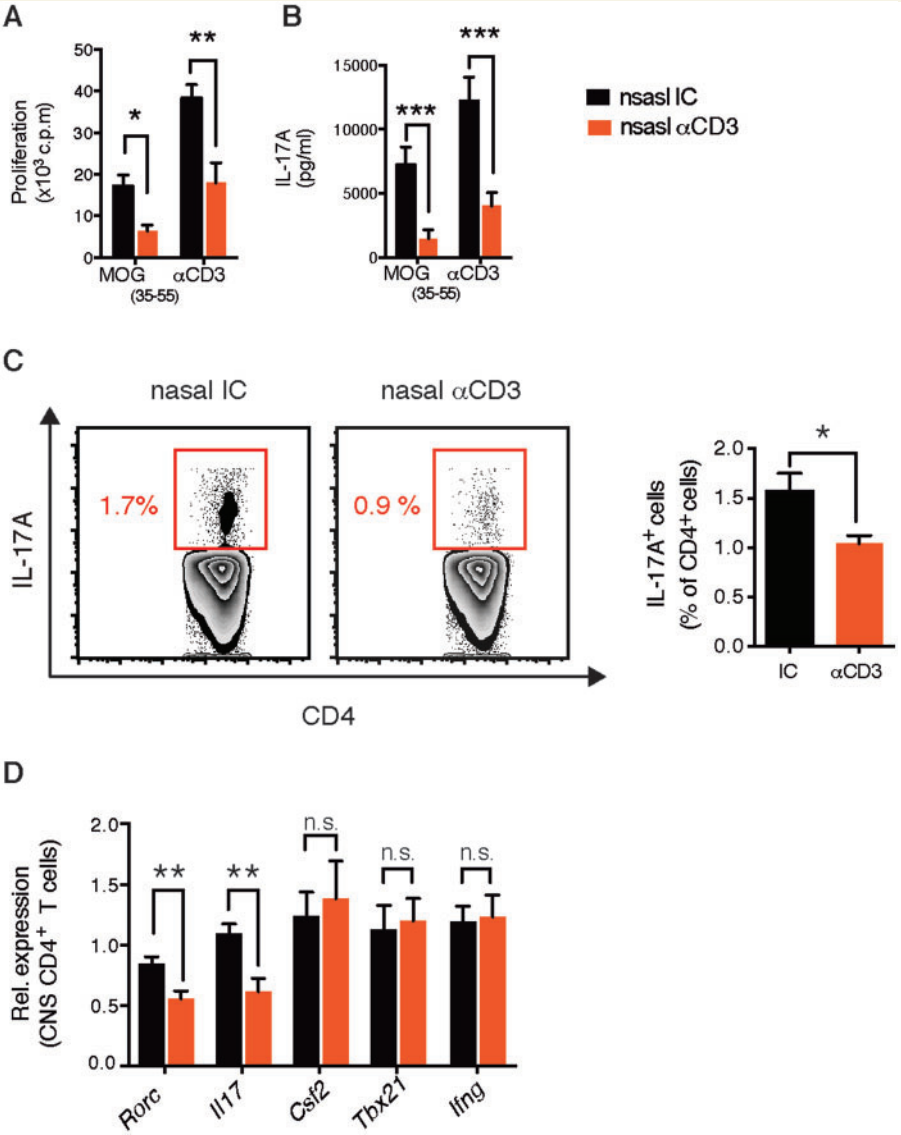

Figure 4 Nasal anti-CD3 attenuates adaptive T-cell responses. Splenic T cell recall response to $MOG_{35–55}$ (20 μg/ml) or anti-CD3 stimulation (0.2 μg/ml); proliferation (**A**) and secretion of the cytokines IL17A (**B**). Data are representative of four independent experiments with $n = 8$ mice/group (mean and SEM). Statistical analysis by Student's *t*-test. (**C** and **D**) EAE NOD mice were treated with CD3 specific or isotype control mAbs during the chronic phase as in Fig. 1A. (**C**) IL17A expression by splenic $CD4^+$ T cells was examined by flow cytometry. (**D**) Quantitative PCR analysis of the expression of *Rorc*, *Il17a*, *Csf2*, *Tbx21*, *and Ifng* mRNA of $CD3^+CD4^+$ T cells isolated from the CNS; expression is presented relative to *Gapdh*. Data are representative of three independent experiments with $n = 6$ mice/group (mean and SEM). Statistical analysis by Student's *t*-test. $^*P < 0.05$, $^{**}P < 0.01$, $^{***}P < 0.001$. n.s. = not significant.

shRNA is driven by a *Gfap* promoter and coupled to a GFP reporter (Fig. 6A). We injected a validated shRNA-encoding lentivirus for *Il10ra* (sh*Il10ra*) or a non-targeting control shRNA (shNT) intra-cerebroventricular during the progressive phase of EAE (35 days after EAE induction) and began nasal anti-CD3 mAb the next day. We confirmed that the expression of the GFP reporter was restricted to $GFAP^+$ astrocytes (Fig. 6B) and that there was significant astrocyte-specific knock-down of *Il10ra* expression (Fig. 6C). As shown in Fig. 6D, knock-down of astrocytic *Il10ra* reversed the therapeutic effects of the nasal anti-CD3. Taken together these data demonstrate the role of IL-10 in astrocytes in nasal anti-CD3 regulation of chronic EAE.

Nasal anti-CD3 monoclonal antibody attenuates microglial activation

Microglia play a central role in the control of CNS inflammation and the progression of EAE (Heppner *et al.*, 2005; Ponomarev *et al.*, 2011; Yamasaki *et al.*, 2014). To investigate the effects of nasal anti-CD3 mAb on microglia, we isolated microglial cells from nasal anti-CD3 mAb treated

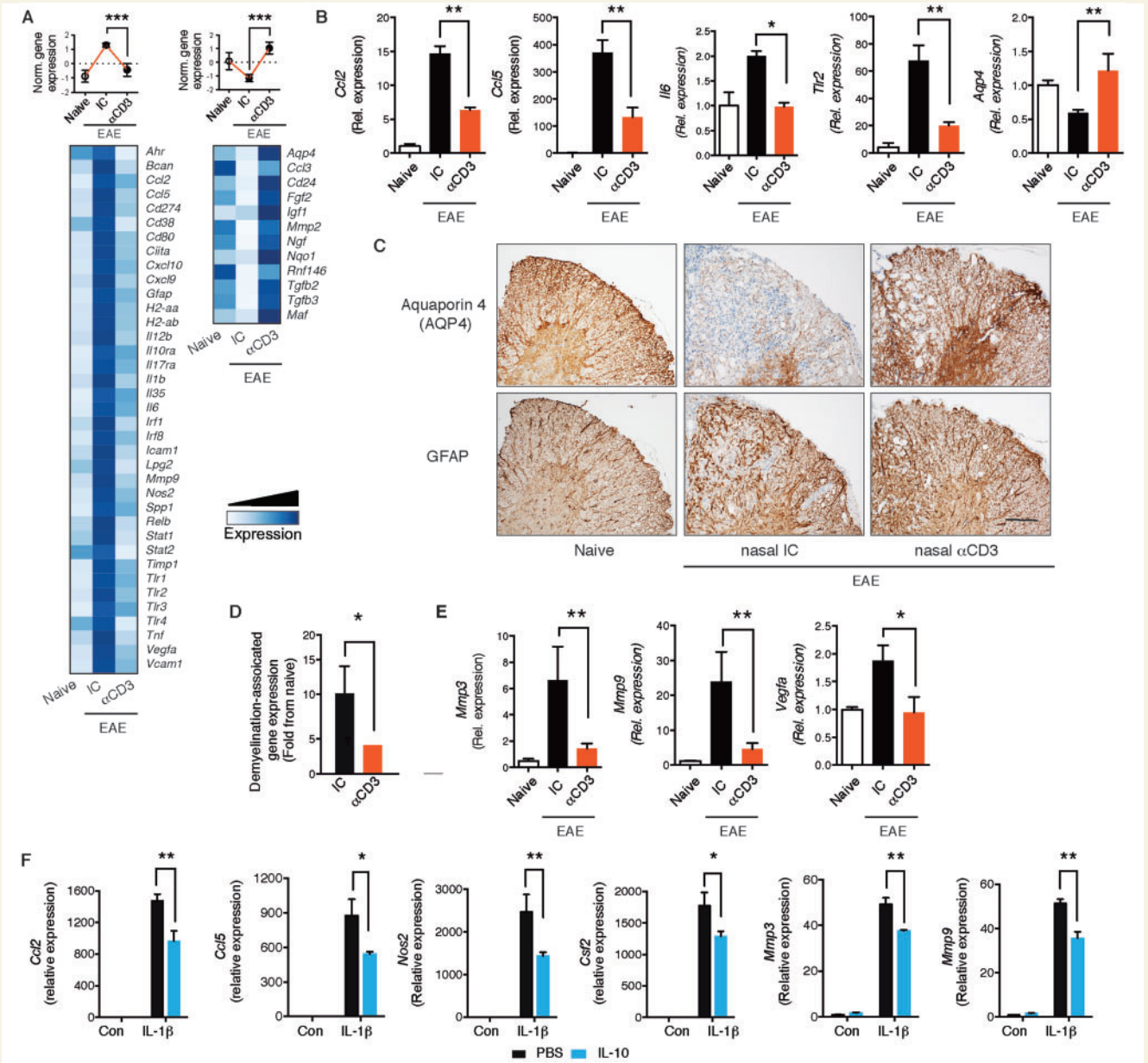

Figure 5 Nasal anti-CD3 suppresses astrocyte activation. (**A–E**) Naïve or EAE NOD mice treated with CD3-specific or isotype control mAbs during the chronic phase as in (Fig. 1A). (**A**) Heat map depicting mRNA expression, as detected by Nanostring nCounter analysis, in astrocytes isolated from naïve or EAE NOD mice treated with CD3 specific or isotype control mAbs. *Upper panels*: Histogram presentation of normalized gene expression in each gene cluster. Representative data of three independent experiments, statistical analysis by one-way ANOVA, followed by Tukey *post hoc* analysis. (**B**) Quantitative PCR analysis of *Ccl2*, *Ccl5*, *Il6*, *Tlr2*, and *Aqp4* expression in astrocytes isolated from naïve and EAE NOD mice treated as in **A**; expression is presented relative to *Gapdh*. Representative data of three independent experiments, statistical analysis by one-way ANOVA, followed by Tukey *post hoc* analysis. (**C**) Immunohistochemistry analysis of spinal cords for aquaporin 4 (AQP4) expression, and the presence of astrocytes (GFAP) on subsequent sections. Scale bar = 50 μm. Data are representative of two independent experiments with $n = 6$ mice/group. (**D**) Relative expression (to NOD naïve group) of genes associated with the control of demyelination in astrocytes isolated from EAE NOD mice treated with anti-CD3 or isotype control. Representative data of three independent experiments. Statistical analysis by Student's *t*-test. (**E**) Quantitative PCR analysis of *Mmp3*, *Mmp9* and *Vegfa* expression in astrocytes isolated from naïve and EAE NOD mice treated as in **A**; expression is presented relative to *Gapdh*. Representative data of three independent experiments, statistical analysis by one-way ANOVA, followed by Tukey *post hoc* analysis. (**F**) Cultured astrocytes were pre-treated for 1 h with IL-10 (100 ng/ml), or vehicle (PBS), followed by activation with IL1β (20 ng/ml) or left untreated. Quantitative PCR analysis of *Ccl2*, *Ccl5*, *Csf2*, *Nos2*, *Mmp3*, and *Mmp9*; expression is presented as fold change from untreated, relative to *Gapdh*. Data from five independent experiments (mean and SEM). Statistical analysis by two-way ANOVA, followed by Tukey *post hoc* analysis. $^{*}P < 0.05$, $^{**}P < 0.01$.

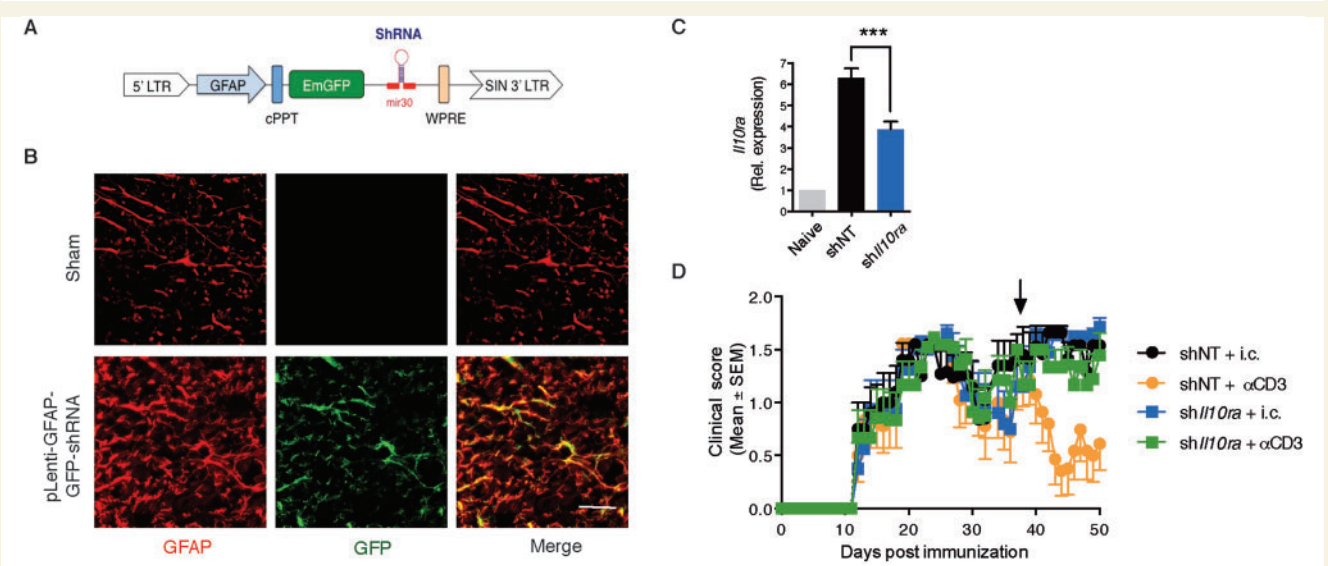

Figure 6 Astrocytic IL-10 receptor has a pivotal role in mediating the therapeutic effect of nasal anti-CD3. (**A**) Schematic map of the astrocyte-specific shRNA lentiviral vector. (**B–D**) Intracerebroventricular injection of astrocyte-specific sh*IL10ra* lentivirus ameliorates disease severity. NOD mice were injected intracerebroventricularly (i.c.v.) with 10^7 IU of shControl, or sh*IL10ra* lentivirus (LV, black arrow), at Day 35 after EAE induction (progressive phase). $n = 10$ mice per group. Two weeks after i.c.v. injection the experiment was terminated and (**B**) immunostaining analysis of spinal cord slices from mock- or lentivirus-infected mice identify GFP^+ expression only in $GFAP^+$ astrocytes. (**C**) *Il10ra* expression levels were determined by quantitative PCR in astrocytes isolated from naïve or EAE NOD mice; expression normalized to *gapdh* and presented relative to that of cells from naïve mice. Representative data of two independent experiments, Statistical analysis by one-way ANOVA, followed by Tukey *post hoc* analysis. (**D**) EAE clinical scores. Representative data of two independent experiments. Statistical analysis by two-way ANOVA. $^{**}P < 0.01$, $^{***}P < 0.001$.

animals and analysed their transcriptional profile using an inflammatory NanoString code set. Nasal anti-CD3 mAb induced both downregulation and upregulation of gene expression in microglia (Fig. 7A). Several of the downregulated genes are known to be associated with microglial activation and we confirmed the downregulation of these genes *(IL1b*, *IL6*, *Nos2*, *Cd40 and Irf7*) by quantitative PCR (Fig. 7B). We then analysed gene expression according to their classification (Krausgruber *et al.*, 2011; Murray and Wynn, 2011) as either 'M1' (pro- inflammatory) or 'M2' (anti-inflammatory) (Supplementary Table 6) and which are also thought to play a role both in multiple sclerosis and EAE (Murray and Wynn, 2011; Miron *et al.*, 2013; Yamasaki *et al.*, 2014). We found that nasal anti-CD3 modulated the microglial phenotype towards an anti-inflammatory pattern (Fig. 7C) with downregulation of M1-associated genes and upregulation of M2-associated genes. Thus, in addition to its effect on astrocytes, nasal anti-CD3 mAb has a profound effect on microglia *in vivo*.

To investigate whether IL-10 acts directly on microglia, we added IL-10 to primary microglial cultures activated with GM-CSF and measured the expression of genes known to play a role in microglial activation and which are associated with an inflammatory microglial phenotype. As shown in Fig. 7D, IL-10 suppressed the response of microglia to recombinant GM-CSF as measured by induction of *Il1b*, *Il6*, *Il12b*, *Cd40*, *Il23a*, and *Tnf*.

To investigate the role of the IL-10-microglial axis on the *in vivo* effect of nasal anti-CD3 mAb, we specifically knocked down *Il10ra* in microglial cells *in vivo*. We used the backbone of the lentivirus-based system described above in Fig. 6. The promoter driving the shRNA expression was replaced with the CD11b promoter (Fig. 7E) to target the microglial cells (Ding *et al.*, 2015). We injected a validated shRNA-encoding lentivirus for *Il10ra* (sh*Il10ra*) or a non-targeting control shRNA (shNT) intraventricularly during the progressive phase of EAE (37 days after EAE induction) and began nasal anti-CD3 mAb treatment the next day. We confirmed that there was significant microglial-specific knock-down of *Il10ra* expression (Fig. 7F). As shown in Fig. 7G, knockdown of microglial *Il10ra* partially reversed the therapeutic effects of the nasal anti-CD3. These data demonstrate that IL-10 acts directly on microglia as well as on astrocytes.

Nasal anti-CD3 monoclonal antibody decreases the recruitment of Ly6Chi monocytes to the central nervous system

CNS-infiltrating monocytes (Ly6Chi) promote neurodegeneration and disease progression in EAE (Izikson *et al.*, 2000; Mildner *et al.*, 2009). As shown above, in

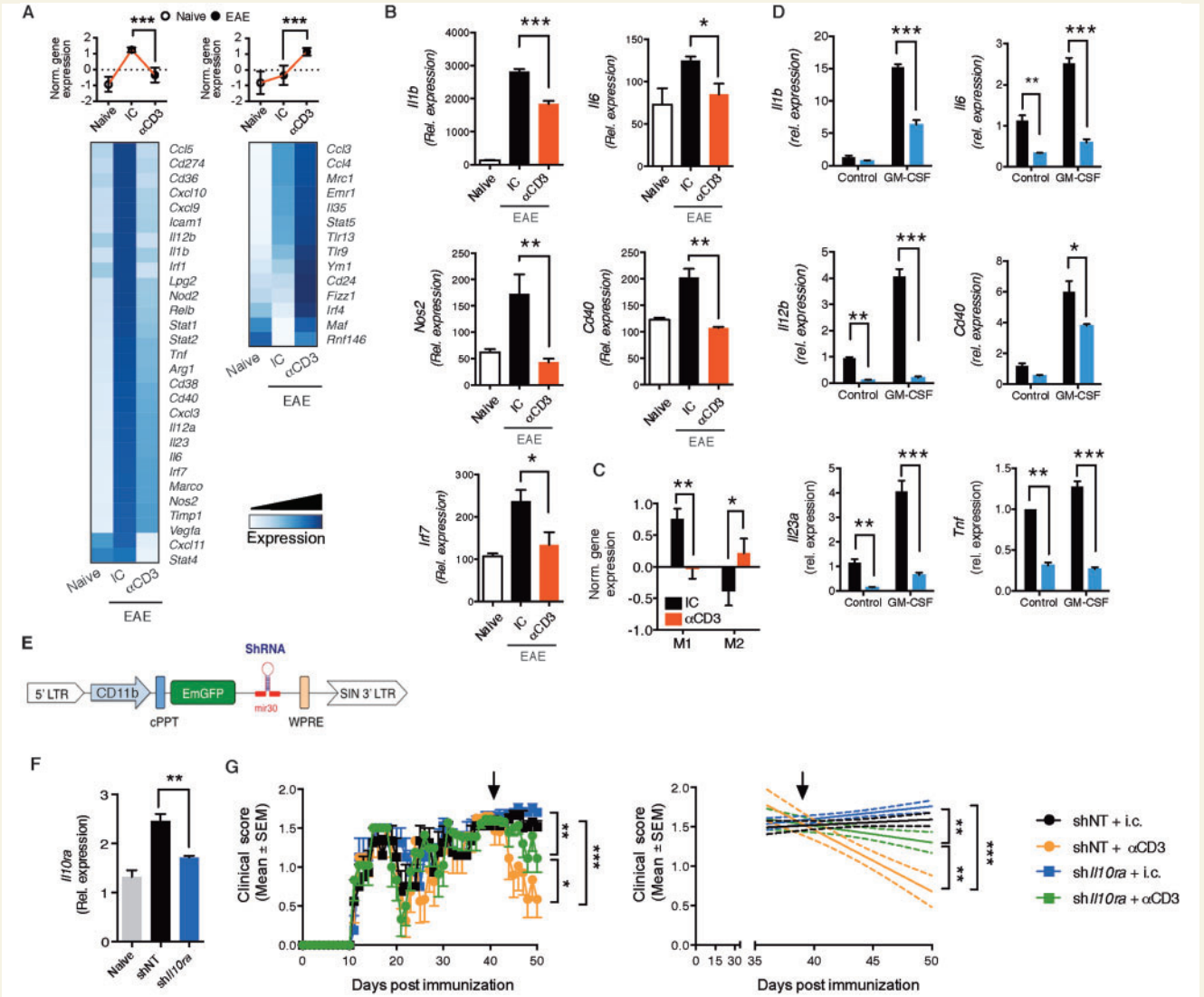

Figure 7 Nasal anti-CD3 attenuates microglial activation. (**A–C**) Naïve or EAE NOD mice treated with CD3 specific or isotype control mAbs during the chronic phase as in Fig. 1A. (**A**) Heat map depicting mRNA expression, as detected by Nanostring nCounter analysis, in microglial cells isolated from naïve or EAE NOD mice treated with CD3 specific or isotype control mAbs. *Upper panels*: Histogram presentation of normalized gene expression in each gene cluster. Representative data of three independent experiments, statistical analysis by one-way ANOVA, followed by Tukey *post hoc* analysis. (**B**) Quantitative PCR analysis of *Il1b*, *Il6*, *Nos2*, *Cd40*, and *Irf7* expression in microglial cells isolated from naïve and EAE NOD mice treated as in **A**; expression is presented relative to *Gapdh*. Representative data of three independent experiments, statistical analysis by one-way ANOVA, followed by Tukey *post hoc* analysis. (**C**) Mean normalized expression of genes associated with M1 or M2 phenotype in microglia (Supplementary Table 6). Statistical analysis by Student's *t*-test. (**D**) Primary microglia were pretreated for 1 h with IL-10 (100 ng/ml), or vehicle (PBS), followed by activation with GM-CSF (25 ng/ml) or left untreated. Quantitative PCR analysis of *Il1b*, *Il6*, *Il12b*, *Cd40*, *H2aa*, and *TNF*; expression is presented as fold-change from untreated relative to *Gapdh*. Data from three independent experiments (mean and SEM). Statistical analysis by Student's *t*-test. $^{*}P < 0.05$, $^{**}P < 0.01$, $^{***}P < 0.001$. (**E–G**) Microglial IL-10 receptor role in mediating the therapeutic effect of nasal anti-CD3. (**E**) Schematic map of the microglia-specific shRNA lentiviral vector. (**F** and **G**) Intracerebroventricular injection of microglia-specific sh*Il10ra* lentivirus ameliorates disease severity. NOD mice were injected i.c.v. with 10^7 IU of shControl, or sh*Il10ra* lentivirus (LV, black arrow), at Day 37 after EAE induction (progressive phase). $n = 10$ mice per group. (**F**) *Il10ra* expression levels were determined by quantitative PCR in microglia isolated from naïve or EAE NOD mice; expression normalized to *Gapdh* and presented relative to that of cells from naïve mice. Representative data of two independent experiments, Statistical analysis by one-way ANOVA, followed by Tukey *post hoc* analysis. (**G**) EAE clinical scores. Representative data of two independent experiments. Statistical analysis by two-way ANOVA. $^{**}P < 0.05$,$^{**}P < 0.01$, $^{***}P < 0.001$.

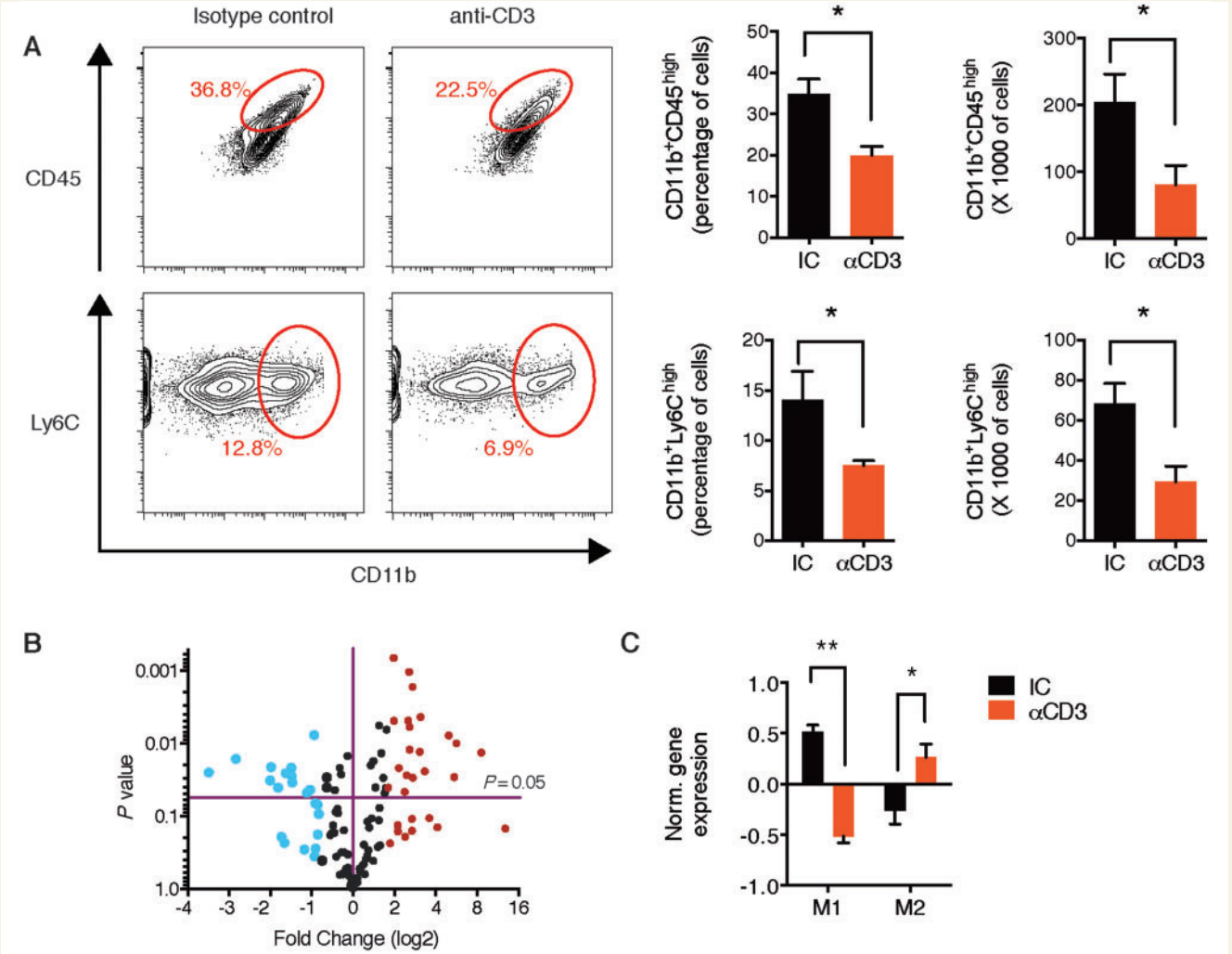

Figure 8 Nasal anti-CD3 decreases the recruitment of Ly6Chi monocytes to the CNS and modulates their phenotype. (**A**) Recruitment of inflammatory monocytes (defined either as of CD11b$^+$Ly6C^{high} or CD11b$^+$CD45^{high} cells) to the CNS NOD EAE mice, treated with CD3 specific or isotype control mAbs during the chronic phase as in Fig. 1A, was analysed by flow cytometry and presented as cell frequency, and total cell numbers. Representative data of three independent experiments. Statistical analysis by Student's *t*-test. (**B**) Volcano plot depicting changes in mRNA expression in CD11b$^+$Ly6C^{high} monocytes isolated from the CNS of NOD EAE mice (as in **A**), as detected by Nanostring nCounter analysis. Changes in gene expression (at least 2-fold) are indicted by colour (Red = increased expression; blue = reduced expression). Representative data of two independent experiments. (**C**) Mean normalized expression of genes associated with M1- or M2-phenotype in microglia (Supplementary Table 6). Statistical analysis by Student's *t*-test. *$P < 0.05$, **$P < 0.01$.

association with reduced expression of *Ccl2* on astrocytes (Fig. 5B), we found that nasal anti-CD3 mAb reduced the infiltration of mononuclear cells to CNS as measured by haematoxylin and eosin staining during the chronic phase on NOD EAE (Fig. 1C). We thus investigated the effect of nasal anti-CD3 mAb on recruitment of inflammatory monocytes (CD11b$^+$Ly6C^{high} and CD11b$^+$CD45^{high} cells) to the CNS, at the same experimental end point. As shown Fig. 8A, we found significant reduction in both the percentages and the total numbers of inflammatory monocytes in the CNS. Of note, no effect on the chemotaxis of monocytes towards CCL2 was observed when monocytes were treated with IL-10 (Supplementary Fig. 6A). However, monocyte migration towards astrocyte-conditioned media was attenuated when astrocytes were pretreated with IL-10 (Supplementary Fig. 6B). Taken together, these data suggest that the anti-CD3 mAb regulation of monocytes recruitment is secondary to the regulation of the astrocyte activation.

In situ reprograming of inflammatory monocytes has been suggested to regulate CNS inflammation (Mayo *et al.*, 2014; Dal-Secco *et al.*, 2015). To determine whether nasal anti-CD3 mAb affected the phenotype of monocytes recruited to the CNS, we isolated CD11b$^+$Ly6C^{high} monocytes from nasal anti-CD3 mAb-treated mice and analysed their transcriptional profile by NanoString nCounter. We found that nasal anti-CD3 mAb significantly altered the monocyte transcriptome (Fig. 8B) by skewing

$CD11b^{+}Ly6C^{high}$ monocytes towards a M2 anti- inflammatory phenotype (Fig. 8C). Thus, nasal anti-CD3 mAb both reduces the recruitment of monocytes to CNS and modulates their immune phenotype.

Discussion

Secondary progressive multiple sclerosis is characterized by continuous and irreversible accumulation of neurological disability (Compston and Coles, 2008; Lassmann *et al.*, 2012) for which there is no effective treatment. The transition to secondary progressive multiple sclerosis has been linked to a change in the nature of CNS inflammation and is thought to be mainly driven by the local innate immune response (Weiner, 2008; Lassmann *et al.*, 2012), which may in turn be associated with abnormalities in the Tr1 cells and changes in the levels of IL-10 (Astier *et al.*, 2007; Kleinewietfeld and Hafler, 2014).

EAE models have been used to study potential treatments for multiple sclerosis. C57BL/6 mice immunized with MOG_{35-55} peptide develop a monophasic disease whereas NOD mice develop a self-limited acute phase followed by an irreversible progressive phase that resembles secondary progressive multiple sclerosis (Basso *et al.*, 2008; Farez *et al.*, 2009; Mayo *et al.*, 2014). The NOD model provides the opportunity to investigate chronic ongoing inflammation and degeneration in the CNS, although, like the acute EAE model there are differences pathologically between these models and the pathological changes observed in subjects with multiple sclerosis.

We found that nasal anti-CD3 mAb induced $IL\text{-}10^{+}LAP^{+}$ regulatory T cells that resemble *in vitro* differentiated Tr1 cells, and suppress progressive EAE in the NOD mouse in an IL-10-dependent manner. Nasal induced-Tr1 cells attenuated the activity of both the adaptive immune response (Th17 cells) and the CNS innate cells—microglia, infiltrating monocytes, and astrocytes. We have previously reported that oral anti-CD3 suppresses acute EAE (Ochi *et al.*, 2006). The mechanism of oral versus nasal anti-CD3 are different as oral anti-CD3 induces TGF-beta secreting cells whereas nasal anti-CD3 induces IL-10 secreting cells. When we directly compared oral versus nasal anti-CD3 in the chronic NOD model we found that oral anti-CD3 did not affect progressive EAE in the NOD mouse (Supplementary Fig. 7), consistent with our present observations that IL-10 is the key mediator of the effects we observed with nasal anti-CD3.

Th17 cells are pro-inflammatory T cells that produce interleukin-17A (IL17A), which is considered a key mediator of chronic tissue inflammation (Baeten and Kuchroo, 2013). Although secondary progressive multiple sclerosis is considered to be primarily driven by the local innate system, IL17 has been associated with progressive multiple sclerosis and elevated levels of IL17-inducible chemokines were found in patients with secondary progressive multiple sclerosis (Baeten and Kuchroo, 2013; Huber *et al.*, 2014). We found that nasal anti-CD3 mAb reduced Th17 polarization, consistent with reports that Tr1 cells regulate Th17 polarization via IL-10 dependent signalling (Huber *et al.*, 2011).

Astrocytes have multiple roles in CNS development and function (Seifert *et al.*, 2006; Tsai *et al.*, 2012; Clarke and Barres, 2013; Mayo *et al.*, 2014), and during CNS inflammation may play different roles affecting blood–brain barrier integrity, axonal growth, monocyte recruitment and the inflammatory milieu of the CNS. We have recently identified a detrimental role for astrocytes during chronic CNS inflammation (Mayo *et al.*, 2014), suggesting that regulating astrocyte activation may be important for the therapy of secondary progressive multiple sclerosis. We found that nasal anti-CD3 mAb attenuated the pro-inflammatory phenotype of astrocytes resulting in the downregulation of genes associated with demyelination, blood–brain barrier degradation (*Vegfa*, *Mmp3*, *Mmp9*), monocyte recruitment (*Ccl2*), and microglial regulation (*Csf2*). Many of these changes could be attributed to the direct regulation by IL-10 of astrocyte activation. Moreover, we demonstrated that knock-down of the astrocytic IL-10 receptor subunit alpha (*Il10ra*), reversed the therapeutic effects of nasal anti-CD3 mAb, suggesting that in progressive EAE, astrocytes represent a main node in the regulation of the inflammatory cascade.

Microglia and CNS-infiltrating inflammatory monocytes ($Ly6C^{high}CCR2^{+}$) are major components of the immune response in the CNS with profound effects on neurodegeneration (Farez *et al.*, 2009; Mildner *et al.*, 2009; Mayo *et al.*, 2012; Miron *et al.*, 2013; Yamasaki *et al.*, 2014). They may acquire different inflammatory phenotypes that have been associated with pro- or anti-inflammatory activities. Pro-inflammatory microglia and monocytes are thought to contribute to the pathogenesis of multiple sclerosis and other CNS disorders (David and Kroner, 2011; Murray and Wynn, 2011). We found that nasal anti-CD3 mAb skewed the microglial and monocyte inflammatory phenotype towards an anti-inflammatory one. We also demonstrated that nasal anti-CD3 mAb attenuated the recruitment of inflammatory monocytes to the CNS, although exogenous IL-10 did not affect monocyte migration toward a CCL2 gradient (the chemokine that governs monocytes recruitment to the CNS in EAE) (Izikson *et al.*, 2000; Mildner *et al.*, 2009) (Supplementary Fig. 5). However, in line with recent studies demonstrating a role for astrocytic-CCL2 production in regulating monocyte recruitment (Kim *et al.*, 2014; Mayo *et al.*, 2014), we found that astrocyte-dependent monocyte migration and CCL2 production are regulated by IL-10. These results suggest that the regulation of monocyte recruitment is secondary to the regulation of astrocyte activation.

A major challenge for the treatment of inflammatory disease is how to induce regulatory T cells in a fashion that is non-toxic and translatable to the clinic setting. Parenteral anti-CD3 mAb is an approved therapy for the treatment of allograft rejection and has been investigated as a treatment for type 1 diabetes (Daifotis *et al.*, 2013). To further study the safety profile of nasal anti-CD3 treatment, we analysed

the *in vivo* distribution of the anti-CD3 mAb and the effect of nasal anti-CD3 on the lung immune system and its response to microbial infection. We found that anti-CD3 mAb accumulated *in vivo* in the cervical lymph nodes in-line with our previous findings that the *in vivo* induction of Tr1 cells by nasal anti-CD3 mAb occurs in the cervical lymph nodes (Wu *et al.*, 2011). Anti-CD3 mAb was not detected in the brain following nasal administration and did not affect the ability of the lung to clear a bacterial infection. Furthermore, nasal anti-CD3 primarily induced MOG-specific Tr1-cells. Should nasal anti-CD3 be tried in human multiple sclerosis, it is likely to have a more benign safety profile than other immunomodulatory treatments as it is triggering a physiologic pathway that has not been targeted before in multiple sclerosis and is stimulating the mucosal immune system rather than disrupting global immune pathways.

In summary, our findings identify nasal anti-CD3 mAb as a therapeutic approach to induce Tr1 type regulatory cells for the treatment of progressive forms of multiple sclerosis and potentially other types of chronic CNS inflammation.

Funding

This work was supported by NIH grants R01AI043458 and P01NS076410 to H.L.W. L.M. is supported by a postdoctoral fellowship (FG1941A1/2) and F.J.Q. is the recipient of a Harry Weaver Award both from the National Multiple Sclerosis Society. Neuropathological studies were in part funded by the Austrian Science Foundation (FWF, Project P 27744-B24).

Supplementary material

Supplementary material is available at *Brain* online.

References

Allan SE, Broady R, Gregori S, Himmel ME, Locke N, Roncarolo MG, et al. CD4+ T-regulatory cells: toward therapy for human diseases. Immunol Rev 2008; 223: 391–421.

Alvarez JI, Dodelet-Devillers A, Kebir H, Ifergan I, Fabre PJ, Terouz S, et al. The Hedgehog pathway promotes blood-brain barrier integrity and CNS immune quiescence. Science 2011; 334: 1727–31.

Anderson AC, Anderson DE, Bregoli L, Hastings WD, Kassam N, Lei C, et al. Promotion of tissue inflammation by the immune receptor Tim-3 expressed on innate immune cells. Science 2007; 318: 1141–3.

Apetoh L, Quintana FJ, Pot C, Joller N, Xiao S, Kumar D, et al. The aryl hydrocarbon receptor interacts with c-Maf to promote the differentiation of type 1 regulatory T cells induced by IL-27. Nat Immunol 2010; 11: 854–61.

Argaw AT, Asp L, Zhang J, Navrazhina K, Pham T, Mariani JN, et al. Astrocyte-derived VEGF-A drives blood- brain barrier disruption in CNS inflammatory disease. J Clin Invest 2012; 122: 2454–68.

Arredouani M, Yang Z, Ning Y, Qin G, Soininen R, Tryggvason K, et al. The scavenger receptor MARCO is required for lung defense against pneumococcal pneumonia and inhaled particles. J Exp Med 2004; 200: 267–72.

Astier AL, Astier AL, Hafler DA, Hafler DA. Abnormal Tr1 differentiation in multiple sclerosis. J Neuroimmunol 2007; 191: 70–8.

Baeten DL, Kuchroo VK. How Cytokine networks fuel inflammation: Interleukin-17 and a tale of two autoimmune diseases. Nat Med 2013; 19: 824–5.

Barrat FJ, Cua DJ, Boonstra A, Richards DF, Crain C, Savelkoul HF, et al. In vitro generation of interleukin 10- producing regulatory CD4(+) T cells is induced by immunosuppressive drugs and inhibited by T helper type 1 (Th1)- and Th2-inducing cytokines. J Exp Med 2002; 195: 603–16.

Basso AS, Frenkel D, Quintana FJ, Costa-Pinto FA, Petrovic-Stojkovic S, Puckett L, et al. Reversal of axonal loss and disability in a mouse model of progressive multiple sclerosis. J Clin Invest 2008; 118: 1532–43.

Clarke LE, Barres BA. Emerging roles of astrocytes in neural circuit development. Nat Rev Neurosci 2013; 14: 311–21.

Compston A, Coles A. Multiple sclerosis. Lancet 2008; 372: 1502–17.

Daifotis AG, Koenig S, Chatenoud L, Herold KC. Anti-CD3 clinical trials in type 1 diabetes mellitus. Clin Immunol 2013; 149: 268–78.

Dal-Secco D, Wang J, Zeng Z, Kolaczkowska E, Wong CH, Petri B, et al. A dynamic spectrum of monocytes arising from the in situ reprogramming of CCR2+ monocytes at a site of sterile injury. J Exp Med 2015; 212: 447–56.

David S, Kroner A. Repertoire of microglial and macrophage responses after spinal cord injury. Nat Rev Neurosci 2011; 12: 388–99.

Ding X, Yan Y, Li X, Li K, Ciric B, Yang J, et al. Silencing IFN-gamma binding/signaling in astrocytes versus microglia leads to opposite effects on central nervous system autoimmunity. J Immunol 2015; 194: 4251–64.

Farez MF, Quintana FJ, Gandhi R, Izquierdo G, Lucas M, Weiner HL. Toll-like receptor 2 and poly(ADP-ribose) polymerase 1 promote central nervous system neuroinflammation in progressive EAE. Nat Immunol 2009; 10: 958–64.

Fitzgerald DC, Zhang G-X, El-Behi M, Fonseca-Kelly Z, Li H, Yu S, et al. Suppression of autoimmune inflammation of the central nervous system by interleukin 10 secreted by interleukin 27–stimulated T cells. Nat Immunol 2007; 8: 1372–9.

Frenkel D, Huang Z, Maron R, Koldzic DN, Hancock WW, Moskowitz MA, et al. Nasal vaccination with myelin oligodendrocyte glycoprotein reduces stroke size by inducing IL10-producing CD4+ T cells. J Immunol 2003; 171: 6549–55.

Han MH, Hwang SI, Roy DB, Lundgren DH, Price JV, Ousman SS, et al. Proteomic analysis of active multiple sclerosis lesions reveals therapeutic targets. Nature 2008; 451: 1076–81.

Heppner FL, Greter M, Marino D, Falsig J, Raivich G, Hovelmeyer N, et al. Experimental autoimmune encephalomyelitis repressed by microglial paralysis. Nat Med 2005; 11: 146–52.

Huber AK, Wang L, Han P, Zhang X, Ekholm S, Srinivasan A, et al. Dysregulation of the IL-23/IL-17 axis and myeloid factors in secondary progressive multiple sclerosis. Neurology 2014; 83: 1500–7.

Huber S, Gagliani N, Esplugues E, O'Connor W Jr, Huber FJ, Chaudhry A, et al. Th17 cells express interleukin-10 receptor and are controlled by Foxp3(-) and Foxp3+ regulatory CD4+ T cells in an interleukin-10-dependent manner. Immunity 2011; 34: 554–65.

Izikson L, Klein RS, Charo IF, Weiner HL, Luster AD. Resistance to experimental autoimmune encephalomyelitis in mice lacking the CC chemokine receptor (CCR)2. J Exp Med 2000; 192: 1075–80.

Kickler K, Ni Choileain S, Williams A, Richards A, Astier AL. Calcitriol modulates the CD46 pathway in T cells. PLoS One 2012; 7: e48486.

Kim RY, Hoffman AS, Itoh N, Ao Y, Spence R, Sofroniew MV, et al. Astrocyte CCL2 sustains immune cell infiltration in chronic experimental autoimmune encephalomyelitis. J Neuroimmunol 2014; 274: 53–61.

Kleinewietfeld M, Hafler DA. Regulatory T cells in autoimmune neuroinflammation. Immunol Rev 2014; 259: 231–44.

Krausgruber T, Blazek K, Smallie T, Alzabin S, Lockstone H, Sahgal N, et al. IRF5 promotes inflammatory macrophage polarization and TH1-TH17 responses. Nat Immunol 2011; 12: 231–8.

Lassmann H, van Horssen J, Mahad D. Progressive multiple sclerosis: pathology and pathogenesis. Nat Rev Neurol 2012; 8: 647–56.

Lock C, Hermans G, Pedotti R, Brendolan A, Schadt E, Garren H, et al. Gene-microarray analysis of multiple sclerosis lesions yields new targets validated in autoimmune encephalomyelitis. Nat Med 2002; 8: 500–8.

Mayo L, Quintana FJ, Weiner HL. The innate immune system in demyelinating disease. Immunol Rev 2012; 248: 170–87.

Mayo L, Trauger SA, Blain M, Nadeau M, Patel B, Alvarez JI, et al. Regulation of astrocyte activation by glycolipids drives chronic CNS inflammation. Nat Med 2014; 20: 1147–56.

Mildner A, Mack M, Schmidt H, Bruck W, Djukic M, Zabel MD, et al. CCR2 + Ly-6Chi monocytes are crucial for the effector phase of autoimmunity in the central nervous system. Brain 2009; 132 (Pt 9): 2487–500.

Miranda-Hernandez S, Baxter AG. Role of toll-like receptors in multiple sclerosis. Am J Clin Exp Immunol 2013; 2: 75–93.

Miron VE, Boyd A, Zhao JW, Yuen TJ, Ruckh JM, Shadrach JL, et al. M2 microglia and macrophages drive oligodendrocyte differentiation during CNS remyelination. Nat Neurosci 2013; 16: 1211–18.

Moore KW, de Waal Malefyt R, Coffman RL, O'Garra A. Interleukin-10 and the interleukin-10 receptor. Ann Rev Immunol 2001; 19: 683–765.

Murray PJ, Wynn TA. Protective and pathogenic functions of macrophage subsets. Nat Rev Immunol 2011; 11: 723–37.

Myer DJ, Gurkoff GG, Lee SM, Hovda DA, Sofroniew MV. Essential protective roles of reactive astrocytes in traumatic brain injury. Brain 2006; 129 (Pt 10): 2761–72.

Nagelhus EA, Ottersen OP. Physiological roles of aquaporin-4 in brain. Physiol Rev 2013; 93: 1543–62.

Nylander A, Hafler DA. Multiple sclerosis. J Clin Invest 2012; 122: 1180–8.

Ochi H, Abraham M, Ishikawa H, Frenkel D, Yang K, Basso AS, et al. Oral CD3-specific antibody suppresses autoimmune encephalomyelitis by inducing CD4 + CD25- LAP + T cells. Nat Med 2006; 12: 627–35.

Petereit HF, Pukrop R, Fazekas F, Bamborschke SU, Ropele S, Kolmel HW, et al. Low interleukin-10 production is associated with higher disability and MRI lesion load in secondary progressive multiple sclerosis. J Neurol Sci 2003; 206: 209–14.

Ponomarev ED, Veremeyko T, Barteneva N, Krichevsky AM, Weiner HL. MicroRNA-124 promotes microglia quiescence and suppresses EAE by deactivating macrophages via the C/EBP-alpha-PU.1 pathway. Nat Med 2011; 17: 64–70.

Prinz M, Priller J, Sisodia SS, Ransohoff RM. Heterogeneity of CNS myeloid cells and their roles in neurodegeneration. Nat Neurosci 2011; 14: 1227–35.

Roncarolo MG, Gregori S, Battaglia M, Bacchetta R, Fleischhauer K, Levings MK. Interleukin-10-secreting type 1 regulatory T cells in rodents and humans. Immunol Rev 2006; 212: 28–50.

Saura J, Tusell JM, Serratosa J. High-yield isolation of murine microglia by mild trypsinization. Glia 2003; 44: 183–9.

Seifert G, Schilling K, Steinhauser C. Astrocyte dysfunction in neurological disorders: a molecular perspective. Nat Rev Neurosci 2006; 7: 194–206.

Soldan SS, Alvarez Retuerto AI, Sicotte NL, Voskuhl RR. Dysregulation of IL-10 and IL-12p40 in secondary progressive multiple sclerosis. J Neuroimmunol 2004; 146: 209–15.

Subramanian A, Tamayo P, Mootha VK, Mukherjee S, Ebert BL, Gillette MA, et al. Gene set enrichment analysis: a knowledge-based approach for interpreting genome-wide expression profiles. Proc Natl Acad Sci USA 2005; 102: 15545–50.

Tsai HH, Li H, Fuentealba LC, Molofsky AV, Taveira-Marques R, Zhuang H, et al. Regional astrocyte allocation regulates CNS synaptogenesis and repair. Science 2012; 337: 358–62.

Ulitsky I, Maron-Katz A, Shavit S, Sagir D, Linhart C, Elkon R, et al. Expander: from expression microarrays to networks and functions. Nat Protoc 2010; 5: 303–22.

van Boxel-Dezaire AH, Hoff SC, van Oosten BW, Verweij CL, Drager AM, Ader HJ, et al. Decreased interleukin- 10 and increased interleukin-12p40 mRNA are associated with disease activity and characterize different disease stages in multiple sclerosis. Ann Neurol 1999; 45: 695–703.

Watkins TA, Emery B, Mulinyawe S, Barres BA. Distinct stages of myelination regulated by gamma-secretase and astrocytes in a rapidly myelinating CNS coculture system. Neuron 2008; 60: 555–69.

Weiner HL. A shift from adaptive to innate immunity: a potential mechanism of disease progression in multiple sclerosis. J Neurol 2008; 255 (Suppl 1): 3–11.

Weiner HL, da Cunha AP, Quintana F, Wu H. Oral tolerance. Immunol Rev 2011; 241: 241–59.

Wingerchuk DM, Carter JL. Multiple sclerosis: current and emerging disease-modifying therapies and treatment strategies. Mayo Clin Proc 2014; 89: 225–40.

Wu HY, Center EM, Tsokos GC, Weiner HL. Suppression of murine SLE by oral anti-CD3: inducible CD4 + CD25- LAP + regulatory T cells control the expansion of IL-17 + follicular helper T cells. Lupus 2009; 18: 586–96.

Wu HY, Maron R, Tukpah A-M, Weiner HL. Mucosal anti-CD3 monoclonal antibody attenuates collagen-induced arthritis that is associated with induction of LAP + regulatory T cells and is enhanced by administration of an emulsome-based Th2-skewing adjuvant. J Immunol 2010; 185: 3401–7.

Wu HY, Quintana FJ, da Cunha AP, Dake BT, Koeglsperger T, Starossom SC, et al. In vivo induction of Tr1 cells via mucosal dendritic cells and AHR signaling. PLoS One 2011; 6: e23618.

Wu HY, Quintana FJ, Weiner HL. Nasal anti-CD3 antibody ameliorates lupus by inducing an IL-10-secreting CD4 + CD25- LAP + regulatory T cell and is associated with down-regulation of IL-17 + CD4 + ICOS + CXCR5 + follicular helper T cells. J Immunol 2008; 181: 6038–50.

Yamasaki R, Lu H, Butovsky O, Ohno N, Rietsch AM, Cialic R, et al. Differential roles of microglia and monocytes in the inflamed central nervous system. J Exp Med 2014; 211: 1533–49.

Yan Y, Ding X, Li K, Ciric B, Wu S, Xu H, et al. CNS-specific therapy for ongoing EAE by silencing IL-17 pathway in astrocytes. Mol Ther 2012; 20: 1338–48.

Yang Z, Chiou TT, Stossel TP, Kobzik L. Plasma gelsolin improves lung host defense against pneumonia by enhancing macrophage NOS3 function. Am J Physiol Lung Cell Mol Physiol 2015; 309: L11–16.